

Holographic entanglement entropy of surface defects

Simon A. Gentle, Michael Gutperle and Chrysostomos Marasinou

*Department of Physics and Astronomy
University of California, Los Angeles, CA 90095, USA*

[sgentle](#), [gutperle](#), cmarasinou@physics.ucla.edu

Abstract

We calculate the holographic entanglement entropy in type IIB supergravity solutions that are dual to half-BPS disorder-type surface defects in $\mathcal{N} = 4$ supersymmetric Yang-Mills theory. The entanglement entropy is calculated for a ball-shaped region bisected by a surface defect. Using the bubbling supergravity solutions we also compute the expectation value of the defect operator. Combining our result with the previously-calculated one-point function of the stress tensor in the presence of the defect, we adapt the calculation of Lewkowycz and Maldacena [1] to obtain a second expression for the entanglement entropy. Our two expressions agree up to an additional term, whose possible origin and significance is discussed.

Contents

1	Introduction	3
2	Review of surface defects in $\mathcal{N} = 4$ SYM	5
3	Review of bubbling supergravity solutions	6
3.1	The vacuum solution	8
3.2	Asymptotics and regularization of the bubbling solution	9
4	Holographic entanglement entropy	10
4.1	Minimal surface geometry	11
4.2	Evaluating the area integral	12
4.3	A 2D CFT interpretation	15
5	Holographic expectation values	17
5.1	$\langle \mathcal{O}_\Sigma \rangle$ calculation	17
5.2	Result and comments	20
5.3	$\langle T_{\mu\nu} \rangle_\Sigma$	21
6	Comparing entanglement entropies	21
7	Discussion	25
A	Fefferman-Graham coordinates	27
A.1	Gauge choice	27
A.2	The coordinate map	28
B	Holographic entanglement entropy	29
C	Coordinate systems and maps	30
D	Asymptotic expansion comparison with [2]	31
E	Holographic expectation value	32
E.1	Bulk term	32
E.2	Gibbons-Hawking term	35

1 Introduction

Entanglement entropy is an important quantity that measures the quantum entanglement between different regions of a system. It furnishes an order parameter for phase transitions and is central to the recent efforts to explore the relation between quantum entanglement and geometry. The Ryu-Takayanagi proposal [3, 4] allows one to calculate entanglement entropies in theories described by a holographic AdS/CFT dual.

The simplest setup for which entanglement entropy can be calculated is a spherical entangling surface in the ground state of a given theory. In recent years many generalizations have been studied both on the field theory side and via holography, including more general entangling surfaces, time dependence, finite temperature and other systems not in their ground state.

Of particular interest is the entanglement entropy in the presence of non-local operators. Two types of non-local operator can be distinguished. Operators such as Wilson lines can be expressed as operator insertions written in terms of the fundamental fields of the theory. However, disorder-type operators cannot be written in this way and are instead characterized by the singular behavior of the fundamental fields close to a defect. One example of the latter is the 't Hooft loop in gauge theories. Note that S -dualities often map defects of the two types into each other [5].

The entanglement entropy for co-dimension one Janus-like defects and boundary CFTs have been studied in [6, 7, 8, 9, 10, 11]. In [12] the entanglement entropy in the presence of defects was related to a thermal entropy on a hyperbolic space, applying the methods of [13] to the presence of a defect.

In [1] the entanglement entropy in the presence of a (supersymmetric) Wilson line operator was calculated in four-dimensional $\mathcal{N} = 4$ $SU(N)$ SYM theory as well as three-dimensional ABJM theories. In the holographically dual theories the description of the Wilson line operator depends on the size of the representation: for representations with Young tableau of order 1, N and N^2 the Wilson line is described by a fundamental string [14, 15], probe D-branes [16, 17, 18] and bubbling supergravity solutions [19]¹, respectively. In [22] the holographic entanglement entropy for the bubbling supergravity solution was computed and exact agreement between the field theory and holographic calculations was found.

Surface operators have received much less attention. In the present paper we focus on disorder-type surface defects in four-dimensional $\mathcal{N} = 4$ $U(N)$ SYM theory constructed in [23, 24]. Their dual description as bubbling geometries of type IIB supergravity was identified in [25] using the solutions constructed in [26, 27]. For notational ease we will drop

¹See [20, 21] for earlier work on bubbling solutions dual to Wilson lines.

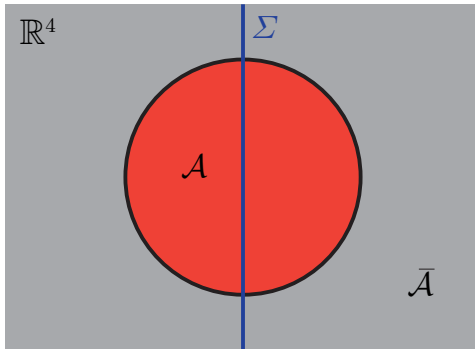


Figure 1: Geometry of the entangling region and surface defect in \mathbb{R}^4 . The entangling region \mathcal{A} is a three-dimensional ball with a two-sphere boundary. The surface defect extends along a spatial line and bisects the two-sphere.

the qualifier ‘disorder-type’ and simply call these ‘surface defects’.

The geometric setup of the surface defect is best visualized in \mathbb{R}^4 . At fixed time the entangling region \mathcal{A} is a three-dimensional ball with a spherical boundary. The surface defect Σ extends in one spatial direction (and time). We depict the setup in figure 1, with one spatial and the time direction suppressed. Note that unlike the case of the Wilson line, it is generic for the surface defect and the boundary of the entangling space to intersect. In the text we also use different geometries, namely $AdS_3 \times S^1$ and $S^1 \times H^3$, which are related to \mathbb{R}^4 by a coordinate change and Weyl rescaling.

The goal of this paper is to calculate the holographic entanglement entropy in the presence of surface defects for $\mathcal{N} = 4$ SYM and compare them to the result obtained by mapping the entanglement entropy to a thermal entropy as in [28]. Here we calculate the expectation values of the surface defect using holography and use the expectation value of the stress tensor that was previously obtained in [2]. The methods used in this paper closely follow those used in our previous paper [29] which addressed the same questions for Wilson surface operators [30, 31, 32] in six-dimensional $(2,0)$ theory [33, 34] and their dual supergravity solutions [35, 36].

The structure of this paper is as follows. In section 2 we review the field theory description of half-BPS surface defects in $\mathcal{N} = 4$ SYM theory. In section 3 we review the bubbling supergravity solutions dual to these defects. In section 4 we calculate the entanglement entropy for a spherical entangling region that intersects the surface defect. In section 5 we calculate the expectation value of the surface defect by evaluating the on-shell supergravity action on the bubbling solution and review the result for the one-point function of the stress energy tensor in the presence of a surface defect. In section 6 the expectation values are used to calculate the entanglement entropy following the method of Lewkowycz and Maldacena [28] which we then compare with our holographic result. The two entanglement

entropies do not match completely and we discuss possible explanations for the mismatch in section 7. Various technical details are presented in the appendices.

2 Review of surface defects in $\mathcal{N} = 4$ SYM

In this section we review the construction of half-BPS surface defects in $\mathcal{N} = 4$ SYM theories first obtained in [23] and studied in detail holographically in [2, 25].

The defects are supported on a two-dimensional surface Σ in \mathbb{R}^4 . They are disorder-type operators so, unlike Wilson line operators, cannot be written as an integral of the fundamental gauge fields over Σ . Instead, they are characterized by singularities of the gauge fields and/or scalar fields at the surface Σ as well as holonomies along cycles in the space normal to the surface. Furthermore, we are interested in half-BPS defects that preserve half the superconformal symmetry $PSU(1, 1|2) \times PSU(1, 1|2)$ inside $PSU(2, 2|4)$. For such superconformal defects it is possible to perform a Weyl transformation from \mathbb{R}^4 to $AdS_3 \times S^1$, in which the surface Σ is mapped to the boundary of AdS_3 . This has two advantages: first, the singularities of the fields along Σ are mapped to boundary behavior in AdS_3 and second, the $AdS_3 \times S^1$ geometry appears naturally in the dual bubbling supergravity solutions that we will review in section 3.

The half-BPS surface defect is characterized by the following data. The non-trivial conditions on the gauge field and scalars break the $U(N)$ gauge group to the Levi subgroup $L = \prod_{i=1}^M U(N_i)$ with M factors. Near the boundary of AdS_3 the gauge field has a non-vanishing component along the $U(1)$ coordinate, which we denote by ψ :

$$A_\psi = \text{diag} \{ \alpha_1 \mathbb{1}_{N_1}, \alpha_2 \mathbb{1}_{N_2}, \dots, \alpha_M \mathbb{1}_{N_M} \} \quad \text{with} \quad \sum_{i=1}^M N_i = N \quad (2.1)$$

There are M theta angles for the M unbroken $U(1)$ factors (see [25, 2] for details), which can be parametrized by the matrix

$$\eta = \text{diag} \{ \eta_1 \mathbb{1}_{N_1}, \eta_2 \mathbb{1}_{N_2}, \dots, \eta_M \mathbb{1}_{N_M} \} \quad (2.2)$$

A complex scalar, which we can choose as $\Phi = \phi_5 + i\phi_6$, has non-trivial behavior along the S^1 :

$$\Phi = \frac{e^{-i\psi}}{\sqrt{2}} \text{diag} \{ (\beta_1 + i\gamma_1) \mathbb{1}_{N_1}, (\beta_2 + i\gamma_2) \mathbb{1}_{N_2}, \dots, (\beta_M + i\gamma_M) \mathbb{1}_{N_M} \} \quad (2.3)$$

To summarize, the surface defect is characterized by the set of M integers N_i and a set of $4M$ real parameters $(\alpha_i, \eta_i, \beta_i, \gamma_i)$ with $i = 1, 2, \dots, M$.

We also cite the results for the expectation value of the surface defect and the one-point function of the stress tensor calculated in [2] in order to compare them with the results of

our holographic calculations. In the semiclassical approximation the expectation value of the surface operator is determined by evaluating the classical $N = 4$ SYM action on the field background. It was shown in [2] that this gives zero and hence

$$\langle \mathcal{O}_\Sigma \rangle = e^{-S_{YM}}|_{\text{surface}} = 1 \quad (2.4)$$

In addition, several one-point functions of local operators and Wilson line operators in the presence of the surface defect were calculated in [2]. The only one which is relevant for the present paper is the one-point function of the stress tensor, which takes the following form due to $AdS_3 \times S^1$ symmetry and the fact that the stress tensor is traceless:

$$\langle T_{\mu\nu} \rangle_\Sigma dx^\mu dx^\nu = h_\Sigma (ds_{AdS_3}^2 - 3 d\psi^2) \quad (2.5)$$

The semiclassical value for the scaling weight h_Σ is found by evaluating the stress tensor of $\mathcal{N} = 4$ SYM on the field background:

$$h_\Sigma = -\frac{2}{3g_{YM}^2} \sum_{i=1}^M N_i (\beta_i^2 + \gamma_i^2) \quad (2.6)$$

3 Review of bubbling supergravity solutions

In [2, 25] it was proposed that the solution found in [26, 27] is the holographic dual of the surface defect operator. The solution is constructed as a $AdS_3 \times S^3 \times U(1)$ fibration over a three-dimensional space with boundary parametrized by the coordinates y, x_1, x_2 , where the boundary is located at $y = 0$. The metric takes the form

$$ds^2 = y \sqrt{\frac{2f+1}{2f-1}} ds_{AdS_3}^2 + y \sqrt{\frac{2f-1}{2f+1}} ds_{S^3}^2 + \frac{2y}{\sqrt{4f^2-1}} (d\chi + V)^2 + \frac{\sqrt{4f^2-1}}{2y} ds_X^2 \quad (3.1)$$

where the AdS_3 metric is in Poincaré coordinates and the metric on the base is simply the flat Euclidean metric:

$$ds_{AdS_3}^2 = \frac{dt^2 + dl^2 + dz^2}{z^2} \quad \text{and} \quad ds_X^2 = (dy^2 + dx_1^2 + dx_2^2) \quad (3.2)$$

The function $f(y, x_1, x_2)$ satisfies a linear partial differential equation with M sources located in the bulk of the base space X at $y = y_i, x = \vec{x}_i$ with $i = 1, 2, \dots, M$:

$$\partial_1^2 f + \partial_2^2 f + y \partial_y \left(\frac{\partial_y f}{y} \right) = \sum_{i=1}^M 2\pi y_i \delta(y - y_i) \delta^2(\vec{x} - \vec{x}_i) \quad (3.3)$$

V is a one-form on X that can be obtained from f by solving

$$dV = \frac{1}{y} \star_3 df \quad (3.4)$$

Note that (3.4) only fixes V up to an exact form and the freedom to redefine $V \rightarrow V + d\omega$ will be important to obtain a manifestly asymptotically AdS metric as detailed in appendix A.1. The only other non-trivial field is the self-dual five-form field strength, which takes the form

$$F_5 = -\frac{1}{4} \left(d \left[y^2 \frac{2f+1}{2f-1} (d\chi + V) \right] - y^3 \star_3 d \left[\frac{f+1/2}{y^2} \right] \right) \wedge \omega_{AdS_3} \\ - \frac{1}{4} \left(d \left[y^2 \frac{2f-1}{2f+1} (d\chi + V) \right] - y^3 \star_3 d \left[\frac{f-1/2}{y^2} \right] \right) \wedge \omega_{S^3} \quad (3.5)$$

where \star_3 denotes the Hodge dual² in the three dimensional base space X with metric given by (3.2).

This solution was first constructed in [27] as a double analytic continuation of the LLM solution [26]. Indeed (3.1) becomes the LLM metric by continuing the $U(1)$ fiber coordinate to a time like coordinate and continuing AdS_3 to S^3 . Note however that the boundary condition on the function f is different: the AdS_3 volume can never shrink to zero size in a smooth solution so we must have $f \rightarrow \frac{1}{2}$ as y approaches the boundary of X . Hence for the bubbling surface solution the coloring of the boundary determined by the regions where $\lim_{y \rightarrow 0} f = \pm \frac{1}{2}$ in the LLM solution gets replaced by the bulk sources in (3.3).

The supergravity solutions depend on $3M$ parameters, which are the M sources on the right hand side of (3.3), located in X at y_i, \vec{x}_i with $i = 1, 2, \dots, M$. There is an overall translation symmetry along \vec{x} ; this allows us to choose ‘center-of-mass’ coordinates, which sets

$$\vec{x}^{(0)} \equiv \sum_{i=1}^M y_i^2 \vec{x}_i = 0 \quad (3.6)$$

This choice will make the expressions considerably more compact. The general solution of (3.3) for the function f is then given by

$$f = \frac{1}{2} + \sum_{i=1}^M f_i \quad (3.7)$$

with

$$f_i = -\frac{1}{2} + \frac{(\vec{x} - \vec{x}_i)^2 + y^2 + y_i^2}{2\sqrt{[(\vec{x} - \vec{x}_i)^2 + y^2 + y_i^2]^2 - 4y^2y_i^2}} \quad (3.8)$$

For such an f the solution of the differential equation (3.4) for the one-form V is given by

$$V_I dx^I = - \sum_{i=1}^M \sum_{I,J} \epsilon_{IJ} \frac{(x_J - x_{iJ})[(\vec{x} - \vec{x}_i)^2 + y^2 - y_i^2]}{2(\vec{x} - \vec{x}_i)^2 \sqrt{[(\vec{x} - \vec{x}_i)^2 + y^2 + y_i^2]^2 - 4y^2y_i^2}} dx^I \quad (3.9)$$

where the indices I, J run over x_1, x_2 .

²The sign of the Hodge dual is fixed by $\star_3 dy = dx_1 \wedge dx_2$ and cyclic permutations of dy, dx_1 and dx_2 .

In [2, 25] the parameters of the supergravity solution were identified with the parameters of the gauge theory surface defect as follows:

$$\frac{1}{2\pi l_s^2} (x_{i1} + ix_{i2}) = \beta_i + i\gamma_i, \quad \frac{y_i^2}{L^4} = \frac{N_i}{N} \quad (3.10)$$

where L denotes the radius of AdS_5 . The parameters α_i and η_i are identified with periods of the NSNS and RR two-form potentials on non-trivial two-cycles in the solutions. On the supergravity side these periods carry only topological information since the three-form field strengths of the two-form potentials vanish. As the calculations performed in section 4 and 5 depend only on the metric and the five-form, we conclude that all our calculations will be independent of the periods and hence the parameters α_i and η_i .

3.1 The vacuum solution

In order to develop intuition for the geometry it is useful to consider the $AdS_5 \times S^5$ vacuum solution, which can be obtained by considering only one source, i.e. setting $M = 1$. Translation invariance allows one to set $\vec{x}_1 = 0$ and from (3.10) we can fix $y_1 = L$ since $N_1 = N$. To exhibit the $AdS_5 \times S^5$ metric explicitly it is convenient to introduce new coordinates:

$$\begin{aligned} \chi &= \frac{1}{2}(\psi - \phi) \\ y &= L^2 \sqrt{\rho^2 + 1} \cos \theta \\ x_1 &= x_1^{(0)} + L^2 \rho \sin \theta \cos(\psi + \phi) \\ x_2 &= x_2^{(0)} + L^2 \rho \sin \theta \sin(\psi + \phi) \end{aligned} \quad (3.11)$$

where the range of the angular variables is given by $\theta \in [0, \pi/2]$, $\psi \in [0, 2\pi]$, $\phi \in [0, 2\pi]$. It is straightforward to verify that for this choice the function f (3.7) and the one-form V (3.9) for the vacuum solution take the following form

$$f = \frac{1}{2} \frac{\rho^2 + \cos^2 \theta + 1}{\rho^2 + \sin^2 \theta} \quad \text{and} \quad V = \frac{1}{2} \frac{\rho^2 - \sin^2 \theta}{\rho^2 + \sin^2 \theta} d(\psi + \phi) \quad (3.12)$$

where the gauge transformation can be set to zero, i.e. $\omega = 0$. Using the expressions given in (3.1) the metric can be calculated and gives

$$ds^2 = L^2 \left[(\rho^2 + 1) ds_{AdS_3}^2 + \frac{d\rho^2}{\rho^2 + 1} + \rho^2 d\psi^2 + d\theta^2 + \sin^2 \theta d\phi^2 + \cos^2 \theta ds_{S^3}^2 \right] \quad (3.13)$$

which is indeed $AdS_5 \times S^5$. Note that the metric is written in a form for which the conformal boundary is $AdS_3 \times S^1$. In the following we will set the AdS radius $L = 1$ and restore it by dimensional analysis when needed.

3.2 Asymptotics and regularization of the bubbling solution

The integrals appearing later in the holographic entanglement entropy and the expectation value calculations are divergent. Therefore, we need to regulate them introducing a cut-off. In this section we map the general metric to a Fefferman-Graham (FG) form (3.19), we find the FG coordinate map (A.6) and derive the cut-off surface (3.20) in terms of the FG UV cut-off.

The fact that a general solution must be asymptotically $AdS_5 \times S^5$ implies the following restriction on y_i :

$$\sum_{i=1}^M y_i^2 = 1 \quad (3.14)$$

It is straightforward to see this considering the map to field theory parameters (3.10) and $\sum_{i=1}^M N_i = N$.

We will work in the coordinate system introduced in (3.11) and expand the general solution at large ρ . As mentioned above, the one-form V is defined up to an exact form. Thus, we use a gauge transformation to remove the V_ρ component of this vector. This brings the metric into a manifestly asymptotic form and makes it as compact as possible which is convenient for our calculations. Fixing the gauge, ω becomes:

$$\omega = -\frac{M-1}{2} \alpha + \sin \theta \sum_{n=1}^{\infty} \frac{V_1^{(n+1)}(\theta, \alpha) \cos \alpha + V_2^{(n+1)}(\theta, \alpha) \sin \alpha}{n \rho^n} \quad (3.15)$$

where the $V_I^{(n+1)}$ are the coefficients in a large ρ expansion of the functions given in (3.9). The detailed procedure and the explicit form of ω are given in the appendix A.1.

The next step is to write the metric in terms of the $\{\rho, \psi, \theta, \phi\}$ coordinates. We write it as a deviation of the vacuum (3.13):

$$\begin{aligned} ds^2 = & \frac{1}{(\rho^2 + 1)} (1 + F_\rho) d\rho^2 + (\rho^2 + 1) (1 + F_1) ds_{AdS_3}^2 + \rho^2 (1 + F_2) d\psi^2 \\ & + \cos^2 \theta (1 + F_3) ds_{S^3}^2 + (1 + F_4) d\theta^2 + \sin^2 \theta (1 + F_5) d\phi^2 \\ & + F_6 d\theta d\psi + F_7 d\psi d\phi + F_8 d\theta d\phi \end{aligned} \quad (3.16)$$

with the F_a being functions of $\{\rho, \theta, \alpha \equiv \psi + \phi\}$ expanded at large ρ . Specifically, $F_\rho, F_m \sim O(\rho^{-2})$ for $m \in \{1, 2, \dots, 7\}$ and $F_8 \sim O(\rho^{-4})$. Only certain coefficients in the F_ρ expansion emerge in our calculations and their expressions are given in the appendix A.2. These coefficients are expressed in terms of dimensionless moments. We will mainly express quantities in terms of these moments throughout the paper and therefore it is convenient to define them in advance:

$$m_{abc} \equiv \sum_{i=1}^M y_i^a x_{i1}^b x_{i2}^c \quad (3.17)$$

Note that for the $AdS_5 \times S^5$ vacuum only the following moments are non-zero:

$$m_{k00}^{(0)} = 1 \quad \text{for} \quad k = 2, 4, 6, \dots \quad (3.18)$$

A general bubbling solution, preserving the $AdS_3 \times S^3 \times S^1$ isometry, can then be written in the following Fefferman-Graham form:

$$ds^2 = \frac{1}{u^2} \left(du^2 + \alpha_1 ds_{AdS_3}^2 + \alpha_2 d\tilde{\psi}^2 \right) + \alpha_3 ds_{S^3}^2 + \alpha_4 d\tilde{\theta}^2 + \alpha_5 d\tilde{\phi}^2 \\ + \alpha_6 d\tilde{\theta} d\tilde{\psi} + \alpha_7 d\tilde{\psi} d\tilde{\phi} + \alpha_8 d\tilde{\theta} d\tilde{\phi} \quad (3.19)$$

The condition that the metric must asymptote to $AdS_5 \times S^5$ with $AdS_3 \times S^1$ boundary implies that the new coordinates $u, \tilde{\psi}, \tilde{\theta}, \tilde{\phi}$ and the α_m (expressed as functions of ρ, ψ, θ, ϕ) fall off as

$$u = \frac{1}{\rho} (1 + \dots), \quad \tilde{\psi} = \psi + \dots, \quad \tilde{\theta} = \theta + \dots, \quad \tilde{\phi} = \phi + \dots \\ \alpha_1 = 1 + \dots, \quad \alpha_2 = 1 + \dots, \quad \alpha_3 = \cos^2 \theta (1 + \dots), \quad \alpha_4 = 1 + \dots \\ \alpha_5 = \sin^2 \theta (1 + \dots), \quad \alpha_6 = \dots, \quad \alpha_7 = \dots, \quad \alpha_8 = \dots$$

The ellipses denote powers of ρ^{-1} whose coefficients are determined by equating (3.16) and (3.19). The explicit coordinate map is given in (A.6).

The integrals in the entanglement entropy and expectation value calculations diverge at large ρ . It is useful to express the coordinate map as a cut-off relation $\rho = \rho_c(\varepsilon, \psi, \theta, \phi)$. This is found by solving the first equation in (A.6) for ρ at the small u limit and identifying u with the FG cut-off, $u = \varepsilon$. The outcome is:

$$\rho_c(\varepsilon, \psi, \theta, \phi) = \frac{1}{\varepsilon} + \frac{F_\rho^{(2)} - 1}{4} \varepsilon + \frac{F_\rho^{(3)}}{6} \varepsilon^2 \\ + \frac{16 \left[F_\rho^{(4)} - F_\rho^{(2)} (F_\rho^{(2)} - 1) \right] - \left(\partial_\theta F_\rho^{(2)} \right)^2 - \left(\partial_\phi F_\rho^{(2)} \right)^2 \csc^2 \theta}{128} \varepsilon^3 + O(\varepsilon^4) \quad (3.20)$$

Once we substitute for the coefficients of F_ρ we find that this function can be written as $\rho_c(\varepsilon, \theta, \alpha)$ with $\alpha = \psi + \phi$.

4 Holographic entanglement entropy

The Ryu-Takayanagi prescription [3, 4] states that the entanglement entropy of a spatial region \mathcal{A} is given by the area of a co-dimension two minimal surface \mathcal{M} in the bulk that is anchored on the $AdS_5 \times S^5$ boundary at $\partial\mathcal{A}$:

$$S_{\mathcal{A}} = \frac{A_{\min}}{4G_N^{(10)}} \quad (4.1)$$

Since we are dealing with static states of our CFT, this surface lies on a constant time slice. If this surface is not unique, we choose the one whose area is minimal among all such surfaces homologous to \mathcal{A} .³

In the following section we derive the minimal surface \mathcal{M} for a general bubbling solution and show that its restriction to the boundary, which is a theory on $AdS_3 \times S^1$, maps to a two-sphere in the Weyl-related \mathbb{R}^4 . We then evaluate its regulated area.

4.1 Minimal surface geometry

A bubbling geometry is a $AdS_3 \times S^3 \times U(1)$ fibration over X . We consider a surface \mathcal{M} at constant t that fills the S^3 and has profile $z = z(l, \chi, y, x_1, x_2)$, where z is the AdS_3 radial coordinate defined in section 3. The induced metric on \mathcal{M} is

$$\begin{aligned} h_{\alpha\beta} dx^\alpha dx^\beta = & y \sqrt{\frac{2f+1}{2f-1}} \frac{1}{z^2} \left[dl^2 + \left(\frac{\partial z}{\partial l} dl + \frac{\partial z}{\partial \chi} d\chi + \frac{\partial z}{\partial y} dy + \frac{\partial z}{\partial x_1} dx_1 + \frac{\partial z}{\partial x_2} dx_2 \right)^2 \right] \\ & + y \sqrt{\frac{2f-1}{2f+1}} ds_{S^3}^2 + \frac{2y}{\sqrt{4f^2-1}} \left[d\chi^2 + 2V_I dx^I d\chi + (V_I dx^I)^2 \right] \\ & + \frac{\sqrt{4f^2-1}}{2y} (dy^2 + dx_1^2 + dx_2^2) \end{aligned} \quad (4.2)$$

where α, β run over all coordinates except t and z . The area functional becomes

$$\begin{aligned} A(\mathcal{M}) = \text{Vol}(S^3) \int dl d\chi dy dx_1 dx_2 \frac{(f - \frac{1}{2})y}{z} \left\{ 1 + \left(\frac{\partial z}{\partial l} \right)^2 + \frac{y^2}{(f - \frac{1}{2})z^2} \left[\left(\frac{\partial z}{\partial y} \right)^2 \right. \right. \\ \left. \left. + \left(\frac{\partial z}{\partial x_1} - V_1 \frac{\partial z}{\partial \chi} \right)^2 + \left(\frac{\partial z}{\partial x_2} - V_2 \frac{\partial z}{\partial \chi} \right)^2 + \frac{(f + \frac{1}{2})(f - \frac{1}{2})}{y^2} \left(\frac{\partial z}{\partial \chi} \right)^2 \right] \right\}^{\frac{1}{2}} \end{aligned} \quad (4.3)$$

The equation of motion that follows from this functional is very complicated, but can be solved by

$$z(l, \chi, y, x_1, x_2)^2 + l^2 = R^2 \quad (4.4)$$

This semicircle is a co-dimension two minimal surface in AdS_3 . Following [12, 9] one can show that within this ansatz this is in fact the surface of minimal area.

The surface (4.4) is independent of the AdS_5 radial coordinate. Thus, the boundary $\partial\mathcal{A}$ of the entangling region on $AdS_3 \times S^1$ satisfies the same formula. To understand this better, let us consider two coordinate charts on \mathbb{R}^4 :

$$ds_{\mathbb{R}^4}^2 = z^2 \left(\frac{dz^2 + dt^2 + dl^2}{z^2} + d\psi^2 \right) = dt^2 + dx^2 + x^2 (d\vartheta^2 + \sin^2 \vartheta d\psi^2) \quad (4.5)$$

³This minimal surface prescription was recently established on a firm footing by the analysis of [28].

The map between these two charts is given by

$$z = x \sin \vartheta, \quad l = x \cos \vartheta \quad (4.6)$$

Thus, our entangling surface $\partial\mathcal{A}$ on the space $AdS_3 \times S^1$ can be written as a two-sphere of radius R on \mathbb{R}^4 (given by $x = R$) upon Weyl rescaling.

4.2 Evaluating the area integral

The minimal area can be written as follows:

$$A_{\min} = \text{Vol}(S^3) \text{Vol}(S^1) \int dl \frac{R}{R^2 - l^2} I \quad (4.7)$$

where we have defined

$$I \equiv \int_X dy dx_1 dx_2 \left(f - \frac{1}{2}\right) y \quad (4.8)$$

with the function f given in (3.7). The area integral, and hence the entanglement entropy, diverges. This is expected due to the infinite number of degrees of freedom localized near the entangling surface and is present even in the vacuum. However, the intersection between the entangling surface and the surface operator leads to an additional divergence. Our goal is to extract the change in entanglement entropy in the presence of the surface operator, which requires a careful treatment of these divergences.

We introduce two independent cut-offs, which we now argue is consistent with our field theory living on $AdS_3 \times S^1$. Firstly, the integral over X diverges due to the infinite volume of AdS_5 . We regulate this with our Fefferman-Graham cut-off ε , which is a UV cut-off on $AdS_3 \times S^1$. Secondly, after using (4.4) to rewrite the l integral as an integral over z , we find a divergence at $z = 0$. This is the location of the surface operator and is at infinite proper distance from other points in the AdS_3 . We therefore interpret this as an IR cut-off and regulate at $z = \eta$.

It is instructive to focus first on the case with no surface operator present in order to exhibit the divergence structure of these integrals most clearly. We begin by changing coordinates via (3.11). Defining $\alpha \equiv \psi + \phi$ and using the vacuum formula (3.12) for f we find

$$I^{(0)} = \int_0^{2\pi} d\alpha \int_0^{\pi/2} d\theta \cos^3 \theta \sin \theta \int_0^{\rho_c^{(0)}} d\rho \rho \quad (4.9)$$

We denote by $\rho_c^{(0)}$ the Fefferman-Graham cut-off function (3.20) evaluated on the vacuum moments (3.18). In this special case it truncates to just two terms and is in fact independent of the angular coordinates: $\rho_c^{(0)} = 1/\varepsilon - \varepsilon/4$. Reinstating the overall factor of L^8 , the full

result for the integral over X is then

$$I^{(0)} = L^8 \left(\frac{\pi}{4\varepsilon^2} - \frac{\pi}{8} + \frac{\pi\varepsilon^2}{64} \right) \quad (4.10)$$

Next we handle the integral over l . Recall that the minimal surface formula (4.4) describes a semicircle for which $z \in [0, R]$ and $l \in [-R, R]$. The l integral diverges at both limits; rewriting via (4.4) as an integral over z , we regulate with a cut-off at $z = \eta$:

$$\begin{aligned} \int_{-\sqrt{R^2-\eta^2}}^{\sqrt{R^2-\eta^2}} dl \frac{R}{R^2-l^2} &= 2 \int_0^{\sqrt{R^2-\eta^2}} dl \frac{R}{R^2-l^2} = 2 \int_{\eta}^R dz \frac{R}{z\sqrt{R^2-z^2}} \\ &= 2 \log \left(\frac{R + \sqrt{R^2-\eta^2}}{\eta} \right) = 2 \log \left(\frac{2R}{\eta} \right) - \frac{\eta^2}{2R^2} + O(\eta^4) \end{aligned} \quad (4.11)$$

To compute the entanglement entropy (4.1) we need the following relations between gravity and gauge theory quantities

$$4G_N^{(10)} = (2\pi)^7 (4\pi)^{-1} g_s^2 \alpha'^4, \quad L^4 = 4\pi g_s N \alpha'^2 \quad (4.12)$$

as well as the volume $\text{Vol}(S^3) = 2\pi^2$. Our final result for the divergent terms of the entanglement entropy in the absence of the surface operator is

$$S_{\mathcal{A}}^{(0)} = N^2 \left[\frac{1}{\varepsilon^2} - \frac{1}{2} + O(\varepsilon^2) \right] \log \left(\frac{2R}{\eta} \right) \quad (4.13)$$

This result looks very different to that for a spherical entangling surface on \mathbb{R}^4 with a single Poincaré-invariant UV cut-off (see [3], for example). The reason is that the AdS_5 boundary in the slicing (3.13) can be reached in two ways: $z \rightarrow 0$ at fixed ρ (the location of the surface defect) or $\rho \rightarrow \infty$ at fixed z (some point away from the defect). We therefore need two cut-offs in this chart.⁴ For a field theory on $AdS_3 \times S^1$, the cut-off η can be viewed as an IR cut-off that regulates the infinite volume of AdS_3 . As we will discuss in some detail in section 6, from the point of view, of the surface defect η should be viewed as a UV cut-off.

Now let us evaluate the area integral in the presence of a surface operator. Our result (4.11) for the integral over l is unchanged. Whilst it is possible to evaluate the integral for I given in (4.8) for a general bubbling geometry after changing coordinates via (3.11), the result is extremely lengthy and cumbersome to deal with. We found the following approach to be much simpler.

For a general bubbling geometry, the integral (4.8) is actually a sum of integrals:

$$I = \sum_{i=1}^M I_i \quad \text{with} \quad I_i \equiv \int_X dy dx_1 dx_2 y f_i \quad (4.14)$$

⁴This situation is also familiar from the $S^1 \times H^{d-1}$ slicing of AdS_{d+1} — see figure 1 of [37], for example.

where the f_i are given in (3.8). We can perform a change of variables for each value of i separately

$$x_1 = y_i \bar{x}_1 + x_{i1}, \quad x_2 = y_i \bar{x}_2 + x_{i2}, \quad y = y_i \bar{y} \quad (4.15)$$

after which the I_i integral becomes

$$I_i = y_i^4 \int_{\bar{X}} d\bar{y} d\bar{x}_1 d\bar{x}_2 \bar{y} f_i \quad \text{with} \quad f_i = -\frac{1}{2} + \frac{\bar{y}^2 + \bar{x}_1^2 + \bar{x}_2^2 + 1}{2\sqrt{(\bar{y}^2 + \bar{x}_1^2 + \bar{x}_2^2 + 1)^2 - 4\bar{y}^2}} \quad (4.16)$$

Now f_i takes the same form as for the vacuum configuration. With a further change of variables the integral can be brought into the same form as (4.9):

$$I_i = y_i^4 \int d\bar{\alpha} d\bar{\theta} d\bar{\rho} \bar{\rho} \cos^3 \bar{\theta} \sin \bar{\theta} \quad (4.17)$$

$$\bar{y} = \sqrt{\bar{\rho}^2 + 1} \cos \bar{\theta}, \quad \bar{x}_1 = \bar{\rho} \sin \bar{\theta} \cos \bar{\alpha}, \quad \bar{x}_2 = \bar{\rho} \sin \bar{\theta} \sin \bar{\alpha} \quad (4.18)$$

All that remains is to impose the correct cut-off in the new variables $\bar{\rho}_c(\varepsilon, \bar{\theta}, \bar{\alpha})$ and then sum up the results for each I_i .

As a side remark, it is interesting that we can express the general integral in the same form as the vacuum. This is because the function f for the general solution is constructed by superimposing terms that each have the same form as the vacuum solution. This simple behavior is special to this system and we do not expect such a simplification to be possible generically.

In order to find $\bar{\rho}_c(\varepsilon, \bar{\theta}, \bar{\alpha})$, our strategy is first to express the unbarred variables $\{\rho, \theta, \alpha\}$ in terms of the barred variables $\{\bar{\rho}, \bar{\theta}, \bar{\alpha}\}$ then to write the FG coordinate u as an asymptotic series in large $\bar{\rho}$. Solving this relation asymptotically for $\bar{\rho}$ and setting $u = \varepsilon$ we obtain the following cut-off function:

$$\begin{aligned} \bar{\rho}_c(\varepsilon, \bar{\theta}, \bar{\alpha}) = & \frac{1}{y_i \varepsilon} - \frac{r_i \cos(\bar{\alpha} + \beta_i) \sin \bar{\theta}}{y_i} + \frac{1}{8y_i} [-1 - 4r_i^2 - 2y_i^2 - 2(y_i^2 - 1) \cos 2\bar{\theta} \\ & - 2m_{220} - 2m_{202} + m_{400} + \sin^2 \bar{\theta} (3 + 2r_i^2 + 2r_i^2 \cos(2\bar{\alpha} + 2\beta_i) \\ & + 6m_{220} + 6m_{202} - 3m_{400} + 12m_{211} \sin 2\bar{\alpha} + 6(m_{220} - m_{202}) \cos 2\bar{\alpha})] \varepsilon \\ & + O(\varepsilon^2) \end{aligned} \quad (4.19)$$

where we have defined $x_{i1} = r_i \cos \beta_i$ and $x_{i2} = r_i \sin \beta_i$. The details on the derivation of the cut-off function $\bar{\rho}_c(\varepsilon, \bar{\theta}, \bar{\alpha})$ are presented in appendix B. Since the coordinate change (4.15) is simply a rescaling followed by a translation, we deduce the following ranges for the integration variables in the I_i integral (4.17):

$$0 \leq \bar{\rho} < \bar{\rho}_c(\varepsilon, \bar{\theta}, \bar{\alpha}), \quad \bar{\theta} \in [0, \pi/2], \quad \bar{\alpha} \in [0, 2\pi] \quad (4.20)$$

We are now ready to evaluate I_i . We perform the $\bar{\rho}$ integral first due to its variable limit. It turns out that the moments drop out in the integration over the angular coordinates. However, they do appear in the final result for I once we sum over i :

$$I = \sum_{i=1}^M I_i = \frac{\pi L^8}{4\varepsilon^2} + \frac{\pi L^8}{24} [1 - 4(m_{220} + m_{202} + m_{400})] + O(\varepsilon) \quad (4.21)$$

where we restored the overall factor of L^8 . As a leading order check we do indeed recover the vacuum result (4.10) when evaluated on the vacuum moments (3.18). The holographic entanglement entropy in the presence of a surface operator (4.1) is evaluated using the minimal area via (4.7) in terms of the two regulated integrals (4.11) and (4.21). At the end, gravity expressions are translated to gauge theory ones using (4.12). Putting all this together, the result is

$$S_{\mathcal{A}} = N^2 \left[\frac{1}{\varepsilon^2} + \frac{1 - 4(m_{220} + m_{202} + m_{400})}{6} + O(\varepsilon) \right] \log \left(\frac{2R}{\eta} \right) \quad (4.22)$$

Subtracting the vacuum contribution from (4.22) and taking $\varepsilon \rightarrow 0$ we arrive at our final result for the change in entanglement entropy due to the presence of a surface operator:

$$\Delta S_{\mathcal{A}} = \frac{2N^2}{3} (1 - m_{220} - m_{202} - m_{400}) \log \left(\frac{2R}{\eta} \right) \quad (4.23)$$

4.3 A 2D CFT interpretation

Let us make a few comments on the form of the result (4.23) for the change in the entanglement entropy. Note immediately that it diverges as $\eta \rightarrow 0$. This additional divergence was anticipated due to the intersection between the entangling surface and the surface defect. The intersection occurs at two points separated by an interval, so it seems natural for the divergence to be logarithmic: our result takes the same form as the entanglement entropy across an interval in the vacuum of a generic two dimensional CFT [38, 39].

Note that the field theory description of the surface operators in section 2 did not require any additional 2D degrees of freedom localized at the surface defect. However, in the original paper [23] an alternative construction of the surface defects by coupling a nonlinear sigma model on Σ to the SYM fields was described. Such a sigma model could describe the 2D CFT we are looking for in the infrared. This construction is based on an intersecting D3-D3' brane system that was first discussed in [40]. Alternatively the defect can be realized by a probe D3-brane in $AdS_5 \times S^5$ with an $AdS_3 \times S^1$ worldvolume. Following Karch and Randall [41] and letting holography ‘act twice’ makes it likely that a 2D CFT is described by the modes on the probe brane.

Consequently it seems possible that the coefficient of the logarithmic divergence in the subtracted entanglement entropy to be equal to (one third of) the central charge of this CFT [38]. We now provide evidence realizing this expectation. Recall that our metric (3.1) takes the form

$$ds^2 = L^2 (e^{2W} ds_{AdS_3}^2 + ds_Z^2) \quad (4.24)$$

We define an effective central charge via the Brown-Henneaux formula [42]:

$$c_{\text{eff}} = \frac{3L}{2G_N^{(3)}} \quad (4.25)$$

where $G_N^{(3)}$ is the three-dimensional Newton's constant of the theory obtained by reducing on the remaining directions in Z . To compute $G_N^{(3)}$ we must take into account the non-trivial warp factor in front of $ds_{AdS_3}^2$:

$$\frac{1}{16\pi G_N^{(3)}} = \frac{1}{16\pi G_N^{(10)}} \Delta \left(\int_Z d^7x \sqrt{g_Z} e^W \right) \quad (4.26)$$

where in order to isolate the contribution from the surface operator we should subtract off the vacuum answer. Substituting the metric (3.1) and reinstating the correct powers of L , our result for the effective central charge via (4.25) is given by

$$c_{\text{eff}} = \frac{3}{2G_N^{(10)}} \text{Vol}(S^3) \text{Vol}(S^1) \Delta I \quad (4.27)$$

where I is the integral (4.8) appearing in the entanglement entropy. From the minimal area prescription (4.1) and integral (4.7) we deduce that

$$\Delta S_{\mathcal{A}} = \frac{c_{\text{eff}}}{3} \log \left(\frac{2R}{\eta} \right) \quad (4.28)$$

which is indeed the entanglement entropy across an interval of length $2R$. Note that from the point of view of the two dimensional CFT the cut-off η is a UV cut-off.

Using (4.27) the central charge c_{eff} can be expressed in terms of the moments

$$c_{\text{eff}} = 2N^2(1 - m_{400} - m_{220} - m_{202}) \quad (4.29)$$

which shows that it scales like N^2 . This is to be contrasted with the sigma model or probe brane construction mentioned above where one would expect that central charge to scale like N^0 or N^1 , respectively. This result makes sense since the holographic supergravity solution is described by a fully back-reacted geometry in which the number of probe branes scales

like N , leading to a number of localized degrees of freedom of order N^2 . It is also instructive to use the map (3.10) to express c_{eff} in terms of field theory quantities:

$$c_{\text{eff}} = 2 \left(N^2 - \sum_{i=1}^M N_i^2 \right) - \frac{8\pi^2}{g_{YM}^2} \sum_{i=1}^M N_i (\beta_i^2 + \gamma_i^2) \quad (4.30)$$

It is intriguing that the first term agrees with the central charge for the sigma model for an $\mathcal{N} = (4, 4)$ two dimensional quiver gauge theory which is related to a pure monodromy defect (where the β_i and γ_i vanish), discussed in [43]. It would be very interesting to explore whether the discussion of [43] can be generalized for nonvanishing β_i and γ_i .⁵

5 Holographic expectation values

This section is devoted to holographic expectation values of different observables. Specifically, we calculate the expectation value of the surface defect \mathcal{O}_Σ at strong coupling and large N . Our result (5.18) is new and is expressed in terms of the moments we introduced in (3.17). We also quote the result of [2] for the holographic one-point function of the stress tensor in the presence of \mathcal{O}_Σ (5.21, 5.22). In section 6 we will make use of these two expectation values in an attempt to relate them to the entanglement entropy computed in section 4.

5.1 $\langle \mathcal{O}_\Sigma \rangle$ calculation

A holographic calculation for the expectation value of the surface operator relies on evaluating the on-shell ten-dimensional type IIB supergravity action on the bubbling supergravity solution presented in section 3. The obstacle here is well-known: it is difficult to reconcile Poincaré invariance of the action with the self-duality condition of the five-form F_5 . Different approaches to this problem have been introduced in the literature: Covariant Lagrangians were constructed with the introduction of an infinite number of auxiliary fields [44, 45, 46, 47, 48, 49, 50], a single auxiliary field in a non-polynomial way [51, 52, 53, 54] and most recently a construction with a free auxiliary four-form field [55]. Formalisms with non-manifest Lorentz symmetry were also considered [56, 57, 58]. The solutions presented in section 3 follow from the standard IIB action where the self-duality constraint (5.2) has to be imposed by hand and not derived from varying the action.

In the holographic approach, the expectation value of the surface operator is given by the on-shell action I :

$$\langle \mathcal{O}_\Sigma \rangle = \exp \left[- (I - I_{(0)}) \right] \quad (5.1)$$

⁵We are grateful to Bruno Le Floch for pointing out reference [43] and useful discussions on the possible relation to our results.

where we subtract off the vacuum contribution $I_{(0)}$. The total action is a sum of a bulk term and the Gibbons-Hawking term:

$$I = I_{\text{bulk}} + I_{\text{GH}} \quad (5.2)$$

$$I_{\text{bulk}} = \frac{1}{2\kappa^2} \left[\int d^{10}x \sqrt{-g} \left(R - \frac{1}{2} \frac{\partial_M \tau \partial^M \bar{\tau}}{(\text{Im } \tau)^2} \right) - \int \left(\frac{1}{2} M_{ab} H_3^a \wedge \star H_3^b + 4F_5 \wedge \star F_5 + \epsilon_{ab} C_4 \wedge H_3^a \wedge H_3^b \right) \right] \quad (5.3)$$

$$I_{\text{GH}} = \frac{1}{\kappa^2} \int d^9x \sqrt{-\gamma} K \quad (5.4)$$

In our case the complex scalar τ field is constant and the three-forms H_3^a vanish. The trace of the equation of motion for the metric implies $R = 0$ and thus the bulk term reduces to

$$I_{\text{bulk}} = -\frac{2}{\kappa^2} \int F_5 \wedge \star F_5 \quad (5.5)$$

To evaluate the bulk term we have to deal with the self-duality of F_5 which when imposed makes (5.5) vanish. In the following we employ a pragmatic method proposed in [59, 60]. The prescription suggests to replace F_5 by its electric part only and double the relevant term in the action. The electric part of F_5 is the component with a time-like leg. As argued in [59, 60] this approach is consistent with Kaluza-Klein reduction and T-duality. It would be interesting to use some of the alternative approaches to deal with the self-dual five-form. This would however imply redoing the derivation of the BPS supergravity solutions in the respective formalism, which is a somewhat daunting task.

Thus, instead of (5.5) we need to evaluate

$$I_{\text{bulk}} = -\frac{4}{\kappa^2} \int F_5^{\text{el.}} \wedge \star F_5^{\text{el.}} \quad (5.6)$$

As the electric part $F_5^{\text{el.}}$ is not self-dual, the integrand of (5.6) does not vanish in general. In particular, since the time coordinate lies in the AdS_3 , the electric part of F_5 in (3.5) consists of the terms that have legs on AdS_3 . It follows from the self-duality of F_5 that the Hodge dual of $F_5^{\text{el.}}$ is the magnetic piece of F_5 , which has legs in S^3 . Consequently we get

$$F_5^{\text{el.}} = -\frac{1}{4} \left(d \left[y^2 \frac{2f+1}{2f-1} (d\chi + V) \right] - y^3 \star_3 d \left[\frac{f+1/2}{y^2} \right] \right) \wedge \omega_{AdS_3} \quad (5.7)$$

$$\star F_5^{\text{el.}} = -\frac{1}{4} \left(d \left[y^2 \frac{2f-1}{2f+1} (d\chi + V) \right] - y^3 \star_3 d \left[\frac{f-1/2}{y^2} \right] \right) \wedge \omega_{S_3} \quad (5.8)$$

Using the equation (3.4) for the one-form V we can write the integrand in (5.6) as

$$F_5^{\text{el.}} \wedge \star F_5^{\text{el.}} = -\frac{yf}{2(1-4f^2)^2} \left[1 - 8f^2 + 16f^4 + \frac{2y}{f} (1-4f^2) \partial_y f \right. \quad (5.9)$$

$$\left. + 4y^2 ((\partial_1 f)^2 + (\partial_2 f)^2 + (\partial_y f)^2) \right] \omega_{AdS_3} \wedge \omega_{S_3} \wedge d\chi \wedge dx_1 \wedge dx_2 \wedge dy \quad (5.10)$$

which can be rewritten in the following way:

$$F_5^{\text{el.}} \wedge \star F_5^{\text{el.}} = \left(-\frac{1}{2} y f + \partial_I u_I + \frac{y^3}{4(1-4f^2)} \left[\partial_1^2 f + \partial_2^2 f + y \partial_y \left(\frac{\partial_y f}{y} \right) \right] \right) \times \omega_{AdS_3} \wedge \omega_{S^3} \wedge d\chi \wedge dx_1 \wedge dx_2 \wedge dy \quad (5.11)$$

where I labels coordinates which run over the base space X , $I = \{x_1, x_2, y\}$ and

$$u_I \equiv -\frac{y^3}{4(1-4f^2)} \partial_I f \quad (5.12)$$

Using the equation (3.3) for f , we can eliminate the final term in (5.11) since its denominator diverges. This is because f diverges at the location of the sources y_i, \vec{x}_i . Thus, the expression for the integrand is given by

$$F_5^{\text{el.}} \wedge \star F_5^{\text{el.}} = \left(-\frac{1}{2} y f + \partial_I u_I(x_1, x_2, y) \right) \omega_{AdS_3} \wedge \omega_{S^3} \wedge d\chi \wedge dx_1 \wedge dx_2 \wedge dy \quad (5.13)$$

The first term appearing in (5.13) includes the holographic entanglement entropy integral (4.8). The last term is a total derivative that can be integrated by applying Stoke's theorem. For the convenience of the reader and completeness we present the evaluation of the integrals for the bulk term in the appendix E.1. The result found in (E.18) is as follows:⁶

$$I_{\text{bulk}} = \frac{\pi}{2\kappa^2} \text{Vol}(AdS_3) \text{Vol}(S^3) \text{Vol}(S^1) \left[\frac{1}{\varepsilon^4} + \frac{1}{\varepsilon^2} + \frac{3}{8} - m_{400} - \mathcal{F} \right] \quad (5.14)$$

where ε is the FG cut-off appearing in (3.20). The final term in the finite piece takes the following form in terms of the moments:

$$\mathcal{F} \equiv \frac{3}{32} \left[1 + 4m_{220} + 4m_{202} - 2m_{400} + 10(m_{220}^2 + m_{202}^2) + 24m_{211}^2 - 4(m_{220} + m_{202})m_{400} + m_{400}^2 - 4m_{220}m_{202} \right] \quad (5.15)$$

The computation of the Gibbons-Hawking term is performed in the appendix E.2. The outcome (E.24) is given by

$$I_{\text{GH}} = \frac{\pi}{2\kappa^2} \text{Vol}(AdS_3) \text{Vol}(S^3) \text{Vol}(S^1) \left(\frac{4}{\varepsilon^4} + \frac{1}{\varepsilon^2} \right) \quad (5.16)$$

We note that the Gibbons-Hawking term does not depend on the moments and is hence independent of the details of the bubbling solution. It is notable that in the analogous calculation of the expectation value for the Wilson surface operator in six-dimensional (2, 0) theories [29] the Gibbons-Hawking term is also independent of the moments.

⁶ \mathcal{F} is identical to the expression $128\Delta\Phi_{2,k}\Delta\Phi_{2,-k}$ with $k = -2, 0, 2$ appearing in [2]. $\Delta\Phi_{2,k}$ are the asymptotic coefficients in a spherical harmonic expansion. Details on this expansion and the relation of $\Delta\Phi_{2,k}$ to our moments can be found in appendix D.

5.2 Result and comments

Now we are ready to put all the pieces together to build the total on-shell action (5.2). Our result is

$$I = \frac{\pi}{2\kappa^2} \text{Vol}(AdS_3) \text{Vol}(S^3) \text{Vol}(S^1) \left[\frac{5}{\varepsilon^4} + \frac{2}{\varepsilon^2} + \frac{3}{8} - m_{400} - \mathcal{F} \right] \quad (5.17)$$

Subtracting the vacuum contribution (which has $m_{400} = 1$), reinstating the overall factor of L^8 and converting to field theory quantities using (4.12) along with $\kappa^2 = 8\pi G_N^{(10)}$, we arrive at our final result for the expectation value:

$$\log \langle \mathcal{O}_\Sigma \rangle = \frac{N^2}{(2\pi)^2} (m_{400} - 1 + \mathcal{F}) \text{Vol}(AdS_3) \text{Vol}(S^1) \quad (5.18)$$

We should compare our holographic result for the expectation value with the semi-classical field theory calculation given in [25]. There, the SYM action was evaluated on $AdS_3 \times S^1$ with the surface defect boundary conditions (2.1) and (2.3) imposed and it was found that $\log \langle \mathcal{O}_\Sigma \rangle = 0$. A field theory interpretation of the holographic result (5.18) in the weak coupling limit is not direct. This is since our result is evaluated using holography and it is valid at strong coupling and large N . Even though the surface operator preserves supersymmetry it is not clear that the holographic results can be trusted at weak coupling. For completeness, however, we make use of the identifications (3.10) and (4.12) to express the moments appearing in (5.18) in terms of field theory quantities:

$$m_{400} = \sum_{i=1}^M \frac{N_i^2}{N^2} \quad (5.19)$$

and

$$\begin{aligned} \frac{\mathcal{F}}{6144} = & \left[\frac{1}{2} - \frac{1}{2N^2} \sum_{i=1}^M N_i^2 + \frac{4\pi^2}{g_{YM}^2 N^2} \sum_{i=1}^M N_i (\beta_i^2 + \gamma_i^2) \right]^2 \\ & + \frac{24\pi^4}{g_{YM}^4 N^4} \sum_{i=1}^M N_i (\beta_i + i\gamma_i)^2 \sum_{j=1}^M N_j (\beta_j - i\gamma_j)^2 \end{aligned} \quad (5.20)$$

The interpretation of \mathcal{F} in the field theory is not clear at this point. One would expect that this term should be a higher order correction to the semi-classical calculation of [25] and it would be interesting to calculate quantum corrections to surface defect operators systematically.

5.3 $\langle T_{\mu\nu} \rangle_\Sigma$

Here we present the stress-energy tensor $\langle T_{\mu\nu} \rangle_\Sigma$ result, evaluated in [2], which we use in the next section. Conformal symmetry constrains the stress-energy tensor form in the presence of the surface defect \mathcal{O}_Σ to (2.5):

$$\langle T_{\mu\nu} \rangle_\Sigma dx^\mu dx^\nu = h_\Sigma (ds_{AdS_3}^2 - 3 d\psi^2) \quad (5.21)$$

$\langle T_{\mu\nu} \rangle_\Sigma$ is preserved and traceless, in line with the fact that Weyl anomaly vanishes for $AdS_3 \times S^1$.

The exact value of h_Σ is calculated in [2] following the holographic renormalization method performed in [61]. We give the dictionary of the result of [2] in terms of the moments (3.17) in appendix D. The final result for h_Σ then takes the following form

$$h_\Sigma = \frac{N^2}{2\pi^2} \left[\frac{1}{16} - \frac{1}{3} \left(m_{220} + m_{202} + \frac{1 - m_{400}}{2} \right) \right] \quad (5.22)$$

6 Comparing entanglement entropies

Our main result in this paper is the subtracted entanglement entropy (4.23) calculated in section 4. The geometric setup is easier to visualize in \mathbb{R}^4 where the spherical entangling surface is a sphere. The setup on \mathbb{R}^4 is related to $AdS_3 \times S^1$ by a diffeomorphism and a Weyl rescaling. We review the various coordinate systems and the geometry of the entangling surface and surface defect in appendix C.

In fact, spherical entangling surfaces are special, since the corresponding modular Hamiltonian is (an integral of) a local operator. In [13], the authors used this fact to write the entanglement entropy across a spherical entangling surface of radius R on $\mathbb{R}^{1,d-1}$ as a thermal entropy on the hyperbolic spacetime $\mathbb{R} \times H^{d-1}$. The latter is conformally related to the causal development of the entangling region on the original Minkowski spacetime.

In [1] this mapping of entanglement entropy to thermal entropy was applied to the calculation of entanglement entropy in the presence of Wilson loops in $\mathcal{N} = 4$ SYM theory and ABJM theories. In particular, it was shown that the additional entanglement entropy due to the presence of the Wilson loop can be calculated from the expectation value of the Wilson loop and the one-point function of the stress tensor. The formula for the additional entanglement entropy due to the presence of a Wilson loop is given by⁷

$$\Delta S = \log \langle W \rangle - \int_{S^1 \times H^{d-1}} d^d x \sqrt{g} \Delta \langle T_{\tau\tau} \rangle_W \quad (6.1)$$

⁷Note that we use the opposite sign convention for the stress tensor from the one used in [1]. Specifically, our convention makes use of the definition $T_{\mu\nu} = \frac{2}{\sqrt{g}} \frac{\delta S}{\delta g^{\mu\nu}}$.

where $\Delta\langle T_{\tau\tau}\rangle_W$ denotes the subtracted (by the one-point function without the Wilson loop inserted) time component of the stress tensor. The two expectation values in (6.1) are calculated on the hyperbolic space $S^1 \times H^{d-1}$, where the coordinate of the thermal circle S^1 is denoted by $\tau \sim \tau + \beta$ with periodicity $\beta = 2\pi R$.

The formula (6.1) is valid for arbitrary representations of the Wilson surface. If the representation becomes very large, i.e. the associated Young tableaux have N^2 boxes, the backreaction on the dual supergravity solution cannot be neglected. This case was examined in [22] by two of the present authors. There, the holographic entanglement entropy was calculated using the bubbling supergravity solutions dual to half-BPS Wilson loops [19]. The expectation values reduce by localization to matrix model integrals [62]. Once matrix model and supergravity solution data are appropriately identified, following [63, 64], it was found that the holographic entanglement entropy exactly agrees with (6.1).

We are also studying a setup with a spherical entangling surface in a CFT, so it is interesting to see whether the same formula (6.1) can be applied to our system. (Of course, the map to a thermal entropy [13] should still hold because the isometry in τ is unbroken.) Here, the Wilson loop operator is replaced by a surface defect. To evaluate (6.1) we have to calculate the values of $\langle \mathcal{O}_\Sigma \rangle$ and the stress tensor on $S^1 \times H^3$. In section 5 we determined them on $AdS_3 \times S^1$, so the first step is map these quantities to the hyperboloid.⁸

Our setup admits a simple description in \mathbb{R}^4 . The three spaces are conformally related as follows:

$$ds_{AdS_3 \times S^1}^2 = z^{-2} ds_{\mathbb{R}^4}^2 = \Omega^2 ds_{S^1 \times H^3}^2 \quad (6.2)$$

where the expressions for the 4D metrics (in the coordinate charts of interest) and the conformal factor Ω are given in (C.1) and (C.3):

$$ds_{S^1 \times H^3}^2 = d\tau^2 + R^2 (d\rho^2 + \sinh^2 \rho (d\vartheta^2 + \sin^2 \vartheta d\psi^2)) \quad \text{and} \quad \Omega^2 = \frac{1}{R^2 \sinh^2 \rho \sin^2 \vartheta} \quad (6.3)$$

For convenience of the reader, further details on the coordinate maps and the description of our setup in these charts is given in appendix C.

It was shown in [65] that even-dimensional surface observables suffer from a conformal anomaly. In particular, the infinitesimal change in the expectation value of \mathcal{O}_Σ is proportional to a linear combination of integrals of the intrinsic and extrinsic curvatures of the surface, whose precise expression is given in equation (2.9) of [2]. The coefficients in this combination depend on the surface operator and the theory and are generically non-zero. However, the

⁸These are the same Euclidean geometry. However, we wish to map a theory quantized on the time t in AdS_3 to a theory quantized on the time τ , so we must perform a non-trivial conformal transformation. Furthermore, the geometric location of the surface defect and the entangling surface is exchanged in the two coordinate systems.

curvature integrals all vanish in our setup of a planar surface at $\partial AdS_3 \subset AdS_3 \times S^1$, so we conclude that $\langle \mathcal{O}_\Sigma \rangle$ is invariant under this conformal transformation. (Of course, the 4D trace anomaly also vanishes on this space, as noted in section 5.3.)

The one-point function of the stress tensor (5.21) transforms in the usual way under a conformal transformation in four dimensions; for example

$$\begin{aligned} \langle \tilde{T}_{\tau\tau} \rangle_\Sigma &= \Omega^2 \left[\left(\frac{\partial t}{\partial \tau} \right)^2 \langle T_{tt} \rangle_\Sigma + \left(\frac{\partial l}{\partial \tau} \right)^2 \langle T_{ll} \rangle_\Sigma + \left(\frac{\partial z}{\partial \tau} \right)^2 \langle T_{zz} \rangle_\Sigma \right] \\ &= \frac{h_\Sigma}{R^4 \sinh^4 \rho \sin^4 \vartheta} \end{aligned} \quad (6.4)$$

where we used the coordinate map from $AdS_3 \times S^1$ to the hyperboloid in (C.4). The full result is traceless as expected since the trace anomaly vanishes on $S^1 \times H^3$:

$$\langle \tilde{T}_{\mu\nu} \rangle_\Sigma d\tilde{x}^\mu d\tilde{x}^\nu = \frac{h_\Sigma}{R^4 \sinh^4 \rho \sin^4 \vartheta} [d\tau^2 + R^2 (d\rho^2 + \sinh^2 \rho (d\vartheta^2 - 3 \sin^2 \vartheta d\psi^2))] \quad (6.5)$$

Note that in even dimensions there is also an inhomogeneous term that generalizes the Schwarzian derivative for the two-dimensional stress tensor. As pointed out in [13, 66] this term does not depend on the state of the theory. Hence it will drop out of the vacuum subtracted stress tensor component $\Delta \langle \tilde{T}_{\tau\tau} \rangle_\Sigma$ in (6.1).

For reasons that will become clear later we write the volume factors in the expression of the expectation value, (5.18), in integral form and change variables. The new variables are the coordinates on the hyperboloid, $\{\tau, \rho, \vartheta, \psi\}$, which have one-to-one map with $AdS_3 \times S^1$ coordinates, $\{t, l, z, \psi\}$. The volume is written as

$$\begin{aligned} \text{Vol}(AdS_3 \times S^1) &= \int_{AdS_3 \times S^1} d^4x \sqrt{g} = \int_{S^1 \times H^3} d^4\tilde{x} \Omega^{-2} \sqrt{\tilde{g}} \\ &= \frac{\beta \text{Vol}(S^1)}{R} \int \frac{d\vartheta}{\sin^3 \vartheta} \int \frac{d\rho}{\sinh^2 \rho} \end{aligned} \quad (6.6)$$

where the integration over ψ and the thermal cycle have been performed. We omit the limits of the integrals over ϑ and ρ to treat them later. Substituting this relation into (5.18) we write the expectation value as

$$\log \langle \mathcal{O}_\Sigma \rangle = N^2 (m_{400} - 1 + \mathcal{F}) \int \frac{d\vartheta}{\sin^3 \vartheta} \int \frac{d\rho}{\sinh^2 \rho} \quad (6.7)$$

The third ingredient in (6.1) is (dropping tildes)

$$\int_{S^1 \times H^3} d^4x \sqrt{g} \Delta \langle T_{\tau\tau} \rangle_\Sigma = (2\pi)^2 \Delta h_\Sigma \int \frac{d\vartheta}{\sin^3 \vartheta} \int \frac{d\rho}{\sinh^2 \rho} \quad (6.8)$$

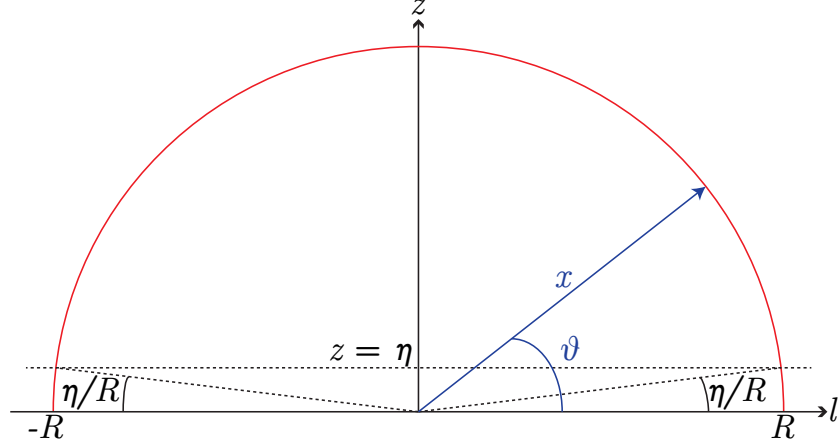


Figure 2: Mapping the $z = \eta$ cut-off to polar coordinates. The red semicircle is the entangling surface while the location of \mathcal{O}_Σ is at $z = 0$. A uniform cut-off $z = \eta$ close to the location of \mathcal{O}_Σ is introduced. It is denoted with a dashed horizontal line. This limits integration over ϑ between η/R and $\pi - \eta/R$.

where Δh_Σ is the vacuum subtracted value of (5.22).

We notice that both ingredients (6.7, 6.8) contain the same integrals. The integrals diverge since the domain of integration is $\vartheta \in [0, \pi]$ and $\rho \in [0, \infty)$. To compute them we introduce two independent cut-offs as follows:

$$\int_{\eta/R}^{\pi-\eta/R} \frac{d\vartheta}{\sin^3 \vartheta} \int_a^\infty \frac{d\rho}{\sinh^2 \rho} = \left[\frac{R^2}{\eta^2} + \log \left(\frac{2R}{\eta} \right) - \frac{1}{6} + O(\eta^2) \right] \left(\frac{1}{a} - 1 + O(a) \right) \quad (6.9)$$

The cut-off η is identified with the homonymous cut-off introduced in the holographic entanglement entropy calculation. The divergence comes from degrees of freedom close to the entangling surface $x = R$. Therefore, for small $z = \eta$ the first map in (C.4) sets the cut-off values of ϑ to η/R and $\pi - \eta/R$ (see figure 2). Since we are interested in the universal term of (6.9) where a is absent, no identification for this cut-off is needed.

We are now ready to combine all the ingredients in (6.1) (with the Wilson loop replaced by the surface defect). The right hand side is

$$\begin{aligned} \log \langle \mathcal{O}_\Sigma \rangle - \int_{S^1 \times H^3} d^d x \sqrt{g} \Delta \langle T_{\tau\tau} \rangle_\Sigma &= \frac{2N^2}{3} \left(1 - m_{220} - m_{202} - m_{400} - \frac{3}{2} \mathcal{F} \right) \log \left(\frac{2R}{\eta} \right) \\ &= \Delta S_{\mathcal{A}} - N^2 \mathcal{F} \log \left(\frac{2R}{\eta} \right) \end{aligned} \quad (6.10)$$

We immediately notice that there is a discrepancy compared to (6.1). The mismatch amounts to the second term in (6.10), which is proportional to \mathcal{F} . The minimal relation (6.1), derived in [1] for Wilson loops, does not work here. This mismatch and possible explanations for it are discussed further in section 7.

7 Discussion

In this paper we studied two-dimensional planar surface defects in $\mathcal{N} = 4$ SYM theory via their dual supergravity bubbling description. First we computed the entanglement entropy across a ball-shaped region bisected by a surface defect. In addition we calculated two other holographic observables: the one-point function of the stress tensor and the expectation value of the surface defect.

We attempted to combine these ingredients as a test of field theory expectations. After a conformal transformation, our entanglement entropy should be equal to the thermal entropy on a hyperbolic space. However, as discussed in section 6, a straightforward generalization of the work of Lewkowycz and Maldacena for Wilson loops [1] did not work in our setup. We now offer some possible reasons for why this is so.

It could be that our cut-off prescription was too naive. However, whilst the sub-leading universal term in (6.9) could receive corrections in a modification of this prescription, the form of the mismatch (characterized by \mathcal{F} in (6.10)) is very different to that of the other terms, so this cannot be the whole story.

The two new elements in our setup compared to [1] were the conformal anomaly for even-dimensional surface observables and the intersection between the entangling surface and the defect. So one possibility is that either element should contribute an extra term to the thermal entropy in addition to those we considered. The same two elements were present in our previous calculations [29] for a Wilson surface in the six-dimensional (2,0) theory. Whilst we do not have a general closed-form expression for the expectation value of the Wilson surface, a case-by-case check yields a similar mismatch. It would be very interesting to pin this down in future work with a direct field theory replica trick calculation.

As discussed for example in [67, 68] there can be an additional contribution to the expectation value of the stress tensor with a defect present which for the case at hand has the general form

$$\langle T_{\mu\nu}(x) \rangle = \langle T_{\mu\nu}^{\text{bulk}}(x) \rangle + \delta^2(x^\perp) \langle T_{\mu\nu}^{\text{defect}}(x) \rangle \quad (7.1)$$

While the bulk contribution to this one point function was given in 5.3, we have not been able to calculate the localized contribution holographically, due to the fact that the standard Fefferman-Graham coordinates break down near the location of the defect as discussed in [12, 69]. We are not aware of any holographic calculation of the defect contribution to the stress tensor in the literature. It would however be very interesting to see whether the extra localized contribution can lead to a match of the two ways to calculate the entanglement entropy presented in this paper. Furthermore, on general grounds the localized term is governed by the Weyl anomaly 'living' on the surface operator and hence such a calculation

would also determine this anomaly holographically.

In order to compute the required thermal entropy, one must compute the free energy in the presence of the defect, which involves taking a derivative with respect to the inverse temperature β . This can be written as a derivative of the field theory Lagrangian with respect to the metric, as utilized in [1]. Whilst the origin of such a term is unclear, it would contribute to the entanglement entropy, so its existence (or lack thereof) should be clear from a replica trick calculation.

Another approach that may provide an understanding of the mismatch is to consider the probe brane approximation, where the defect operator is realized as D3 branes with an $AdS_3 \times S^1$ worldvolume inside $AdS_5 \times S^5$ and the backreaction is neglected or treated perturbatively. The expectation value is known for both types of surface operator [2, 31] and the entanglement entropy can be computed to leading order using the results of [37] (see also [12, 70, 71]). It would be interesting to determine whether the mismatch we found persists in this approximation.

The logarithmic divergence in the entanglement entropy in the vacuum of a 2D CFT is universal: it depends only on the central charge. It is natural to ask whether the coefficient in our subtracted result (4.23) is similarly universal. We computed an effective central charge holographically in section 4.3 and found precise agreement with this coefficient. Indeed, the same agreement is found for the holographic description of a Wilson surface in the $(2, 0)$ theory [29]. It would be very interesting to pursue this connection further and develop a 2D CFT description for both types of surface operator.

Acknowledgements

We are delighted to thank Xi Dong, Matthew Headrick, Bruno Le Floch, Edgar Shaghoulian and Christoph Uhlemann for useful discussions. This work was supported in part by National Science Foundation grant PHY-13-13986. The work of MG was in part supported by a fellowship of the Simons Foundation. MG thanks the Institute for Theoretical Physics, ETH Zürich, for hospitality while this work was in progress.

A Fefferman-Graham coordinates

This section complements the discussion of the FG mapping procedure in section 3. We describe the gauge choice for the one-form V and give the results of the FG coordinate map.

A.1 Gauge choice

As mentioned in section 3 we are interested to choose ω such that $V_\rho = 0$. In particular, we first need to expand the function

$$\omega = \sum_{n=0}^{\infty} \frac{\omega^{(n)}(\theta, \alpha)}{\rho^n} \quad (\text{A.1})$$

where $\alpha = \psi + \phi$ and demand that $V_\rho = 0$ at each order in the ρ^{-1} expansion. This is a gauge choice that kills all $d\rho dY$ cross terms with $Y \in \{\psi, \theta, \phi\}$ in the asymptotic expansion of the metric⁹. Then we fix $\omega^{(0)}$ by demanding that the $d\theta d\psi$ and $d\psi d\phi$ cross terms vanish at zeroth order for all M . Considering the expansion of the one-form (3.9) at large ρ :

$$V_I = \sum_{n=1}^{\infty} \frac{V_I^{(n)}(\theta, \alpha)}{\rho^n} \quad (\text{A.2})$$

The result for ω is given in terms of $V_I^{(n)}$ coefficients in (3.15). Substituting the explicit expressions for the coefficients it can be written as

$$\begin{aligned} \omega = & -\frac{M-1}{2} \alpha + \frac{1}{2 \sin \theta \rho} \sum_{i=1}^M (x_{i2} \cos \alpha - x_{i1} \sin \alpha) \\ & - \frac{1}{4 \sin^2 \theta \rho^2} \sum_{i=1}^M [(x_{i1}^2 - x_{i2}^2) \sin 2\alpha - 2x_{i1}x_{i2} \cos 2\alpha] \\ & - \frac{1}{6 \sin^3 \theta \rho^3} \sum_{i=1}^M [(x_{i1}^3 - 3x_{i1}x_{i2}^2) \sin 3\alpha + (x_{i2}^3 - 3x_{i1}^2x_{i2}) \cos 3\alpha] \\ & + \frac{1}{8\rho^4} \left\{ \frac{1}{\sin^4 \theta} \sum_{i=1}^M [4(x_{i1}^3x_{i2} - x_{i1}x_{i2}^3) \cos 4\alpha - (x_{i1}^4 - 6x_{i1}^2x_{i2}^2 + x_{i2}^4) \sin 4\alpha] \right. \\ & \left. + \sin^2 \theta \sum_{i=1}^M [-8y_i^2x_{i1}x_{i2} \cos 2\alpha + 4(y_i^2x_{i1}^2 - y_i^2x_{i2}^2) \sin 2\alpha] \right\} + O(\rho^{-5}) \quad (\text{A.3}) \end{aligned}$$

This is the gauge choice which eliminates the V_ρ component and brings the metric in a manifestly asymptotically $AdS_5 \times S^5$ form.

⁹Note that ds_X^2 defined in (3.2) has no $d\rho dY$ cross terms.

A.2 The coordinate map

In this subsection we give the results of the FG mapping. We express them in terms of the expansion coefficients of the functions F_a appearing in (3.16). The coefficients relevant to our calculation come from the expansion of F_ρ :

$$F_\rho = \sum_{n=1}^{\infty} \frac{F_\rho^{(n)}(\theta, \alpha)}{\rho^n} \quad (\text{A.4})$$

In what follows we express the relevant coefficients in terms of the moments:

$$\begin{aligned} 4F_\rho^{(2)} &= (1 - 3 \cos 2\theta) [1 + 2(m_{220} + m_{202}) - m_{400}] \\ &\quad + 12 [\cos 2\alpha (m_{220} - m_{202}) + 2m_{211} \sin 2\alpha] \sin^2 \theta \\ F_\rho^{(3)} &= 3 (\sin \theta - \sin 3\theta) [(m_{212} + m_{230} - m_{410}) \cos \alpha + (m_{221} + m_{203} - m_{401}) \sin \alpha] \\ &\quad + 4 \sin^3 \theta [(-3m_{212} + m_{230}) \cos 3\alpha - (-3m_{221} + m_{203}) \sin 3\alpha] \\ 32F_\rho^{(4)} &= -4 \cos^4 \theta + (5 - 12 \cos 2\theta + 15 \cos 4\theta) (2m_{202} + 2m_{220} - m_{400}) \\ &\quad - 16 (1 + 5 \cos 2\theta) \sin^2 \theta \sin 2\alpha [3m_{211} + 8(m_{213} + m_{231}) - 12m_{411}] \\ &\quad - 8 (1 + 5 \cos 2\theta) \sin^2 \theta \cos 2\alpha [3(m_{220} - m_{202}) + 8(m_{240} - m_{204}) + 12(m_{402} - m_{420})] \\ &\quad - 640 \sin 4\alpha \sin^4 \theta (m_{213} - m_{231}) + 24 (3 - 4 \cos 2\theta + 5 \cos 4\theta - 40 \cos 4\alpha \sin^4 \theta) m_{222} \\ &\quad + 4 (9 - 12 \cos 2\theta + 15 \cos 4\theta + 40 \cos 4\alpha \sin^4 \theta) (m_{204} + m_{240}) \\ &\quad - 4 (3 - 4 \cos 2\theta + 5 \cos 4\theta) [6(m_{402} + m_{420}) - m_{600}] \\ &\quad - \left(12 \sin^2 \theta [\cos 2\alpha (m_{202} - m_{220}) - 2 \sin 2\alpha m_{211}] \right. \\ &\quad \left. - (1 - 3 \cos 2\theta) (2m_{202} + 2m_{220} - m_{400}) \right)^2 \end{aligned} \quad (\text{A.5})$$

The FG mapping, as described in section 3, gives the following results for the FG coordinates:

$$\begin{aligned} u &= \frac{1}{\rho} \left[1 + \frac{F_\rho^{(2)} - 1}{4\rho^2} + \frac{F_\rho^{(3)}}{6\rho^3} + \frac{16(F_\rho^{(4)} - F_\rho^{(2)} + 1) - (\partial_\theta F_\rho^{(2)})^2 - (\partial_\phi F_\rho^{(2)})^2 \csc^2 \theta}{128\rho^4} + O(\rho^{-5}) \right] \\ \tilde{\psi} &= \psi - \frac{\partial_\psi F_\rho^{(2)}}{16\rho^4} - \frac{\partial_\psi F_\rho^{(3)}}{30\rho^5} + O(\rho^{-6}) \\ \tilde{\theta} &= \theta - \frac{\partial_\theta F_\rho^{(2)}}{8\rho^2} - \frac{\partial_\theta F_\rho^{(3)}}{18\rho^3} + \frac{1}{256\rho^4} [-8\partial_\theta F_\rho^{(4)} + 3\partial_\phi F_\rho^{(2)} \partial_\theta \partial_\phi F_\rho^{(2)} \csc^2 \theta \\ &\quad - (\partial_\phi F_\rho^{(2)})^2 \cot \theta \csc^2 \theta + \partial_\theta F_\rho^{(2)} (12 - 4F_\rho^{(2)} + 16F_4^{(2)} + 3\partial_\theta^2 F_\rho^{(2)})] + O(\rho^{-5}) \\ \tilde{\phi} &= \phi - \frac{\partial_\phi F_\rho^{(2)}}{8 \sin^2 \theta \rho^2} - \frac{\partial_\phi F_\rho^{(3)}}{18 \sin^2 \theta \rho^3} + \frac{1}{256 \sin^2 \theta \rho^4} [-8\partial_\phi F_\rho^{(4)} + 3\partial_\theta F_\rho^{(2)} \partial_\theta \partial_\phi F_\rho^{(2)} \\ &\quad + \partial_\phi F_\rho^{(2)} (12 - 4F_\rho^{(2)} + 16F_5^{(2)} + 3\partial_\phi^2 F_\rho^{(2)} \csc^2 \theta - 4\partial_\theta F_\rho^{(2)} \cot \theta)] + O(\rho^{-5}) \end{aligned} \quad (\text{A.6})$$

B Holographic entanglement entropy

In this section we present some details of the holographic entanglement entropy calculation performed in section 4. To compute the integrals (4.14) involved in the area functional we performed a change of variables (4.15) which brought the integrals to a form matching the vacuum integrals (4.17). To set the limits of integration over $\bar{\rho}$ we need to express the FG cut-off in the new coordinates as $\bar{\rho}_c(\bar{\theta}, \bar{\alpha}, \varepsilon)$.

The first step is to express $\{\rho, \theta, \alpha\}$ coordinates in terms of $\{\bar{\rho}, \bar{\theta}, \bar{\alpha}\}$. Combining (3.11, 4.15, 4.18) we can write the change of variables as

$$\begin{aligned}\sqrt{\rho^2 + 1} \cos \theta &= y_i \sqrt{\bar{\rho}^2 + 1} \cos \bar{\theta} \\ \rho \sin \theta \cos(\alpha) &= y_i \bar{\rho} \sin \bar{\theta} \cos \bar{\alpha} + r_i^2 \cos^2 \beta_i \\ \rho \sin \theta \sin(\alpha) &= y_i \bar{\rho} \sin \bar{\theta} \sin \bar{\alpha} + r_i^2 \sin^2 \beta_i\end{aligned}\tag{B.1}$$

where we have defined $x_{i1} = r_i \cos \beta_i$ and $x_{i2} = r_i \sin \beta_i$. We begin with solving the first equation in terms of ρ . Then, we combine the last two equations to eliminate α and we substitute ρ . This gives an equation for $\sin \theta$ in terms of the barred variables:

$$\sin^4 \theta + A \sin^2 \theta + B = 0\tag{B.2}$$

with

$$\begin{aligned}A &= -1 + r_i^2 + 2\bar{\rho} r_i y_i \cos(\bar{\alpha} - \beta_i) \sin \bar{\theta} + \frac{y_i^2 (1 + \cos 2\bar{\theta} + 2\bar{\rho}^2)}{2} \\ B &= -r_i^2 - 2\bar{\rho} r_i y_i \cos(\bar{\alpha} - \beta_i) \sin \bar{\theta} + \frac{\bar{\rho}^2 y_i^2 (\cos 2\bar{\theta} - 1)}{2}\end{aligned}\tag{B.3}$$

Since $\theta \in [0, \pi/2]$ we choose the solution for which $\sin \theta$ is real and positive. We get the rest by plugging this solution into the equations (B.1). Specifically, ρ is found by plugging $\sin \theta$ into the first equation while $\sin \bar{\alpha}$ and $\cos \bar{\alpha}$ are found using the other two equations. Since

we only need the asymptotic behavior we give the results expanded at large $\bar{\rho}$:

$$\begin{aligned}
\rho^2 &= y_i^2 \bar{\rho}^2 + 2r_i y_i \cos(\bar{\alpha} + \beta_i) \sin \bar{\theta} \bar{\rho} + \frac{1}{2} (y_i^2 + 2r_i^2 - 1 + (y_i^2 - 1) \cos 2\bar{\theta}) + O\left(\frac{1}{\bar{\rho}}\right) \\
\sin^2 \theta &= \sin^2 \bar{\theta} + \frac{2r_i \cos(\bar{\alpha} + \beta_i) \cos^2 \bar{\theta} \sin \bar{\theta}}{y_i \bar{\rho}} \\
&\quad + \frac{\cos^2 \bar{\theta} (1 - y_i^2 + (y_i^2 + 2r_i^2 - 1) \cos 2\bar{\theta} - 4r_i^2 \cos(2\bar{\alpha} + 2\beta_i) \sin^2 \bar{\theta})}{2y_i^2 \bar{\rho}^2} + O\left(\frac{1}{\bar{\rho}^3}\right) \\
\sin \alpha &= \sin \bar{\alpha} + \frac{r_i \csc \bar{\theta} (\cos \beta_i - \cos(\bar{\alpha} + \beta_i) \sin \bar{\alpha})}{y_i \bar{\rho}} \\
&\quad + \frac{r_i^2 \csc^2 \bar{\theta} (-4 \cos \beta_i \cos(\bar{\alpha} + \beta_i) + \sin \bar{\alpha} + 3 \cos(2\bar{\alpha} + 2\beta_i) \sin \bar{\alpha})}{4y_i^2 \bar{\rho}^2} + O\left(\frac{1}{\bar{\rho}^3}\right) \\
\cos \alpha &= \cos \bar{\alpha} - \frac{r_i \csc \bar{\theta} (\cos \beta_i + \cos(2\bar{\alpha} + \beta_i) - 2 \sin \beta_i)}{2y_i \bar{\rho}} \\
&\quad + \frac{r_i^2 \csc^2 \bar{\theta} (-4 \sin \beta_i \cos(\bar{\alpha} + \beta_i) + \cos \bar{\alpha} + 3 \cos(2\bar{\alpha} + 2\beta_i) \cos \bar{\alpha})}{4y_i^2 \bar{\rho}^2} + O\left(\frac{1}{\bar{\rho}^3}\right) \quad (\text{B.4})
\end{aligned}$$

To find the cut-off $\bar{\rho}_c(\bar{\theta}, \bar{\alpha}, \varepsilon)$ we substitute (B.4) in the expression for the FG coordinate u , which can be found in (A.6), to get u in terms of the barred coordinates.

$$\begin{aligned}
u &= \frac{1}{y_i \bar{\rho}} - \frac{r_i \cos(\bar{\alpha} + \beta_i) \sin \bar{\theta}}{y_i^2 \bar{\rho}^2} - \frac{1}{8y_i^3 \bar{\rho}^3} \left[1 + 4r_i^2 + 2y_i^2 + 2(y_i^2 - 1) \cos 2\bar{\theta} \right. \\
&\quad + 2m_{220} + 2m_{202} - m_{400} - 3 \sin^2 \bar{\theta} (1 + 2r_i^2 + 2r_i^2 \cos(2\bar{\alpha} + 2\beta_i) \\
&\quad \left. + 2m_{220} + 2m_{202} - m_{400} + 4 \sin 2\bar{\alpha} m_{211} + 2 \cos 2\bar{\alpha} (m_{220} - m_{202})) \right] + O\left(\frac{1}{\bar{\rho}^4}\right) \quad (\text{B.5})
\end{aligned}$$

Solving this asymptotically for $\bar{\rho}$ and setting $u = \varepsilon$ we find the cut-off surface in barred coordinates.

$$\begin{aligned}
\bar{\rho}_c(\varepsilon, \bar{\theta}, \bar{\alpha}) &= \frac{1}{y_i \varepsilon} - \frac{r_i \cos(\bar{\alpha} + \beta_i) \sin \bar{\theta}}{y_i} + \frac{1}{8y_i} \left[-1 - 4r_i^2 - 2y_i^2 - 2(y_i^2 - 1) \cos 2\bar{\theta} \right. \\
&\quad - 2m_{220} - 2m_{202} + m_{400} + \sin^2 \bar{\theta} (3 + 2r_i^2 + 2r_i^2 \cos(2\bar{\alpha} + 2\beta_i) \\
&\quad \left. + 6m_{220} + 6m_{202} - 3m_{400} + 12 \sin 2\bar{\alpha} m_{211} + 6 \cos 2\bar{\alpha} (m_{220} - m_{202})) \right] \varepsilon + O(\varepsilon^2) \quad (\text{B.6})
\end{aligned}$$

C Coordinate systems and maps

In this section we collect useful formulae for the various coordinate systems and their maps along with information about our setup in these systems. In particular we relate $AdS_3 \times S^1$ to $S^1 \times H^3$ with an intermediate transformation to \mathbb{R}^4 . In the latter space the picture of our setup becomes more clear (see figure 1).

The metrics on the 4D Euclidean spaces we consider are the following:

$$\begin{aligned}
AdS_3 \times S^1 & \quad ds_{AdS_3 \times S^1}^2 = \frac{dt^2 + dl^2 + dz^2}{z^2} + d\psi^2 \\
\text{spherical} & \quad ds_{\mathbb{R}^4}^2 = dt^2 + dx^2 + x^2 (d\vartheta^2 + \sin^2 \vartheta d\psi^2) \\
\text{hyperboloid} & \quad ds_{S^1 \times H^3}^2 = d\tau^2 + R^2 (d\rho^2 + \sinh^2 \rho (d\vartheta^2 + \sin^2 \vartheta d\psi^2))
\end{aligned} \tag{C.1}$$

They are conformally related to each other as follows:

$$ds_{AdS_3 \times S^1}^2 = z^{-2} ds_{\mathbb{R}^4}^2, \quad ds_{\mathbb{R}^4}^2 = \bar{\Omega}^2 ds_{S^1 \times H^3}^2, \quad ds_{AdS_3 \times S^1}^2 = \Omega^2 ds_{S^1 \times H^3}^2 \tag{C.2}$$

where

$$\bar{\Omega} = (\cosh \rho + \cos(\tau/R))^{-1}, \quad \Omega = (R \sinh \rho \sin \vartheta)^{-1} \tag{C.3}$$

The coordinate maps corresponding to these three transformations are given by

$$\begin{aligned}
AdS_3 \times S^1 \text{ to spherical: } & l = x \cos \vartheta, \quad z = x \sin \vartheta \\
\text{spherical to hyperboloid: } & t = R \bar{\Omega} \sin(\tau/R), \quad x = R \bar{\Omega} \sinh \rho \\
AdS_3 \times S^1 \text{ to hyperboloid: } & t = R \bar{\Omega} \sin(\tau/R), \quad l = R \bar{\Omega} \sinh \rho \cos \vartheta, \quad z = R \bar{\Omega} \sinh \rho \sin \vartheta
\end{aligned} \tag{C.4}$$

where the last transformation comes from combining the first two.

For easy reference we quote the location Σ of the surface defect and the location $\partial\mathcal{A}$ of the entangling surface in the various coordinate charts:

	Σ	$\partial\mathcal{A}$
$AdS_3 \times S^1$	fills t , fills $l, z = 0$	$t = 0, l^2 + z^2 = R^2$
spherical	fills t , fills $x, \vartheta = 0, \pi$	$t = 0, x = R$
hyperboloid	fills τ , fills $\rho, \vartheta = 0, \pi$	$\rho \rightarrow \infty$

It can be seen, in all coordinate charts, that the surface defect intersects the entangling surface exactly at two points.

D Asymptotic expansion comparison with [2]

For calculating holographic observables one has to expand the supergravity solution in an asymptotic form. In this section we quote the way the asymptotic expansion was performed in [2] and compare with ours.

Defining $\Phi = f/y$ the equation for f , (3.3), can be written as the six-dimensional Laplace equation for Φ with $SO(4)$ invariant sources. In [2] the authors write Φ as the vacuum part and a deviation:

$$\Phi = \Phi^{(0)} + \Delta\Phi \tag{D.1}$$

Then, they expand the deviation $\Delta\Phi$ in $SO(4)$ -invariant spherical harmonics. The coefficients of this expansion are denoted by $\Delta\Phi_{\Delta,k}$, where Δ, k are eigenvalues characterizing the spherical harmonics (for more details on the spherical harmonics see appendix A in [2]).

As an example, we quote their result for the one-point function of the stress tensor which was found using holography:

$$\langle T_{\mu\nu} \rangle_{\Sigma} dx^{\mu} dx^{\nu} = \frac{N^2}{2\pi^2} \left(\frac{1}{16} - \frac{1}{12\sqrt{3}} \Delta\Phi_{2,0} \right) (ds_{AdS_3}^2 - 3 d\psi^2) \quad (\text{D.2})$$

One can see that this matches (5.21, 5.22), when a definition for $\Delta\Phi_{2,0}$ is given in terms of the moments. For completeness we give all the coefficients corresponding to spherical harmonics with eigenvalue $\Delta = 2$ in terms of the moments:

$$\begin{aligned} \Delta\Phi_{2,0} &= 4\sqrt{3} \left(m_{220} + m_{202} + \frac{1 - m_{400}}{2} \right) \\ \Delta\Phi_{2,\pm 2} &= 6e^{\mp 2i\psi} (m_{220} - m_{202} \pm 2im_{211}) \end{aligned} \quad (\text{D.3})$$

E Holographic expectation value

In this appendix we compute the integrals involved in the expectation value of the surface defect (5.1). Specifically, these are the bulk contribution given in (5.6) and the Gibbons-Hawking term in (5.4).

E.1 Bulk term

Let us start with the evaluation of the bulk term. The method described in [59, 60] led us to (5.11) the integrand of which we expressed as (5.13). We begin with carrying out the integration over AdS_3 , S^3 and S^1 , which is trivial. Then, the bulk term can be expressed in terms of two integrals over the base space X :

$$I_{\text{bulk}} = -\frac{4}{\kappa^2} \text{Vol}(AdS_3) \text{Vol}(S^3) \text{Vol}(S^1) \left[-\frac{1}{2} J_1 + J_2 \right] \quad (\text{E.1})$$

where we have defined:

$$J_1 = \int_X dx_1 dx_2 dy f y \quad (\text{E.2})$$

$$J_2 = \int_X dx_1 dx_2 dy \partial_I u_I \quad (\text{E.3})$$

Making use of the integral (4.8) appearing in the entanglement entropy calculation we

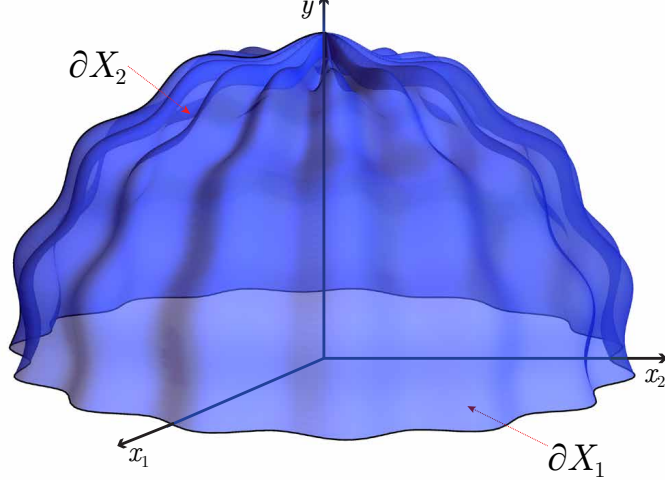


Figure 3: The base space X boundary components: the blue wiggled dome noted as ∂X_2 is the large ρ cut-off and the lowest flat surface noted as ∂X_1 is the boundary at the x_1, x_2 plane.

can write

$$J_1 = \int_X dx_1 dx_2 dy \left[\left(f - \frac{1}{2} \right) y + \frac{1}{2} y \right] \quad (\text{E.4})$$

$$= \frac{\pi}{4\epsilon^2} + \frac{\pi}{24} [1 - 4(m_{220} + m_{202} + m_{400})] + \frac{1}{2} \int_X dx_1 dx_2 dy y \quad (\text{E.5})$$

where we have dropped terms that vanish as $\epsilon \rightarrow 0$. The integral in the second line can be evaluated directly by changing to $\{\rho, \theta, \alpha\}$ coordinates (the relevant map is given in (3.11)):

$$\begin{aligned} \int_X dx_1 dx_2 dy y &= \int d\rho d\theta d\alpha \rho (\rho^2 + \sin^2 \theta) \cos \theta \sin \theta \\ &= \int_0^{\pi/2} d\theta \int_0^{2\pi} d\alpha \frac{1}{4} \rho^2 (\rho^2 + 2 \sin^2 \theta) \cos \theta \sin \theta \Big|_0^{\rho_c(\epsilon, \theta, \alpha)} \\ &= \frac{\pi}{4\epsilon^4} + \frac{\pi}{16\epsilon^2} (1 + 2m_{220} + 2m_{202} - m_{400}) + Y_1 \end{aligned} \quad (\text{E.6})$$

where the term Y_1 reads:

$$\begin{aligned} Y_1 &\equiv \frac{\pi}{768} [-7 + 12m_{220} + 12m_{202} - 6m_{400} \\ &\quad - 288(m_{220}^2 + m_{202}^2) + 144m_{220}m_{202} - 720m_{211}^2 + 108(m_{220} + m_{202})m_{400} - 27m_{400}^2 \\ &\quad + 48(m_{240} + m_{204}) + 96(m_{222} - m_{402} - m_{420}) + 16m_{600}] \end{aligned} \quad (\text{E.7})$$

Next we evaluate J_2 by turning it into an integral over the boundary of X . Switching to

covariant notation in which g_{IJ} is a metric on X we have

$$J_2 = \int_X d^3x \sqrt{g} \nabla_I u^I \quad (\text{E.8})$$

$$= \int_{\partial X} d^2x \sqrt{\gamma} n_I u^I \quad (\text{E.9})$$

where n is the outward-pointing unit normal vector and γ the induced metric on ∂X . This surface consists of two components (see figure 3):

$$\partial X_1 = \{(x_1, x_2, y) | y = 0, x_1^2 + x_2^2 \leq \rho_c(\varepsilon, \pi/2, \alpha)^2\} \quad (\text{E.10})$$

$$\partial X_2 = \{(\rho, \theta, \alpha) | \rho = \rho_c(\varepsilon, \theta, \alpha), \theta \in [0, \pi/2], \alpha \in [0, 2\pi]\} \quad (\text{E.11})$$

The contribution to J_2 from ∂X_1 vanishes. This can be easily seen by expanding (5.12) for small y and take the $y \rightarrow 0$ limit. For the remaining contribution we work in $\{\rho, \theta, \alpha\}$ coordinates. The metric on X is

$$ds_X^2 = \frac{\rho^2 + \sin^2 \theta}{\rho^2 + 1} d\rho^2 + (\rho^2 + \sin^2 \theta) d\theta^2 + \rho^2 \sin^2 \theta d\alpha^2 \quad (\text{E.12})$$

The unit vector normal to the surface $\rho - \rho_c(\varepsilon, \theta, \alpha) = 0$ has the following components in this chart:

$$n_\rho = \frac{1}{\mathcal{D}}, \quad n_\theta = -\frac{\partial_\theta \rho_c(\varepsilon, \theta, \alpha)}{\mathcal{D}}, \quad n_\alpha = -\frac{\partial_\alpha \rho_c(\varepsilon, \theta, \alpha)}{\mathcal{D}} \quad (\text{E.13})$$

$$\mathcal{D} \equiv \sqrt{\frac{[\partial_\alpha \rho_c(\varepsilon, \theta, \alpha)]^2}{\rho^2 \sin^2 \theta} + \frac{\rho^2 + 1 + [\partial_\theta \rho_c(\varepsilon, \theta, \alpha)]^2}{\rho^2 + \sin^2 \theta}} \quad (\text{E.14})$$

The induced metric and pullback components are given by

$$\gamma_{ab} = g_{IJ} e_a^I e_b^J \quad \text{with} \quad e_a^I = \begin{pmatrix} \partial_\theta \rho_c(\varepsilon, \theta, \alpha) & \partial_\alpha \rho_c(\varepsilon, \theta, \alpha) \\ 1 & 0 \\ 0 & 1 \end{pmatrix} \quad (\text{E.15})$$

where $a \in \{\theta, \alpha\}$. We are now ready to evaluate J_2 :

$$\begin{aligned} J_2 &= \int_0^{\pi/2} d\theta \int_0^{2\pi} d\alpha \sqrt{\gamma} \frac{y^3}{4(4f^2 - 1)} g^{IJ} n_I \partial_J f \\ &= -\frac{\pi}{16\varepsilon^4} + \frac{\pi}{64\varepsilon^2} (1 + 2m_{220} + 2m_{202} - m_{400}) + Y_2 \end{aligned} \quad (\text{E.16})$$

where

$$\begin{aligned} Y_2 &\equiv \frac{\pi}{3072} [-51 - 100m_{220} - 100m_{202} + 50m_{400} \\ &\quad + 72(m_{220}^2 + m_{202}^2) + 144m_{211}^2 - 36(m_{220} + m_{202})m_{400} + 9m_{400}^2 \\ &\quad + 48(m_{240} + m_{204}) + 96(m_{222} - m_{402} - m_{420}) + 16m_{600}] \end{aligned} \quad (\text{E.17})$$

Putting everything together we get

$$I_{\text{bulk}} = \frac{\pi}{2\kappa^2} \text{Vol}(AdS_3) \text{Vol}(S^3) \text{Vol}(S^1) \left[\frac{1}{\varepsilon^4} + \frac{1}{\varepsilon^2} + \frac{3}{8} - m_{400} + \frac{2}{\pi} (Y_1 - 4Y_2) \right] \quad (\text{E.18})$$

Plugging in the explicit expressions for Y_1 and Y_2 we notice that the moments of weight six drop out. The result is given in (5.14, 5.15).

E.2 Gibbons-Hawking term

To compute the Gibbons-Hawking term (5.4) we use a similar method to that used in the previous subsection for the total derivative on X , but now in the full ten-dimensional space-time. The unit vector normal to the surface $\rho - \rho_c(\varepsilon, \theta, \alpha) = 0$ has the following non-trivial components

$$n_\rho = \frac{1}{\mathcal{D} \sqrt{\frac{2y}{\sqrt{4f^2-1}}}}, \quad n_\theta = -\frac{\partial_\theta \rho_c(\varepsilon, \theta, \alpha)}{\mathcal{D} \sqrt{\frac{2y}{\sqrt{4f^2-1}}}}, \quad n_\alpha = -\frac{\partial_\alpha \rho_c(\varepsilon, \theta, \alpha)}{\mathcal{D} \sqrt{\frac{2y}{\sqrt{4f^2-1}}}} \quad (\text{E.19})$$

where \mathcal{D} is defined in (E.14). The induced metric and non-trivial pullback components are given by

$$\gamma_{ab} = g_{MN} e_a^M e_b^N \quad (\text{E.20})$$

$$e_\theta^\rho = \partial_\theta \rho_c(\varepsilon, \theta, \alpha), \quad e_\alpha^\rho = \partial_\alpha \rho_c(\varepsilon, \theta, \alpha), \quad e_b^a = \delta_b^a \quad (\text{E.21})$$

where now a runs over all coordinates except ρ . The extrinsic curvature can be computed from the Lie derivative along n :

$$K_{ab} = \frac{1}{2} (\mathcal{L}_n g)_{MN} e_a^M e_b^N \quad (\text{E.22})$$

$$= \frac{1}{2} (n^P \partial_P g_{MN} + g_{PN} \partial_M n^P + g_{MP} \partial_N n^P) e_a^M e_b^N \quad (\text{E.23})$$

and its trace is simply $K \equiv \gamma^{ab} K_{ab}$ (whose small ε expansion leads with order 4). The result is

$$I_{\text{GH}} = \frac{\pi}{2\kappa^2} \text{Vol}(AdS_3) \text{Vol}(S^3) \text{Vol}(S^1) \left(\frac{4}{\varepsilon^4} + \frac{1}{\varepsilon^2} \right) \quad (\text{E.24})$$

The moments appearing in the boundary integrand drop out when the integration over the angles $\{\theta, \alpha\}$ is performed.

Note that there is in principle a contribution from the other component of the boundary at $y = 0$, but again this vanishes. Specifically, expanding the Gibbons-Hawking integrand for small y we get $\sqrt{\gamma} K = O(y^2)$ which vanishes in the $y \rightarrow 0$ limit.

References

- [1] A. Lewkowycz and J. Maldacena, “Exact results for the entanglement entropy and the energy radiated by a quark,” *JHEP* **05** (2014) 025, [arXiv:1312.5682 \[hep-th\]](#).
- [2] N. Drukker, J. Gomis, and S. Matsuura, “Probing N=4 SYM With Surface Operators,” *JHEP* **10** (2008) 048, [arXiv:0805.4199 \[hep-th\]](#).
- [3] S. Ryu and T. Takayanagi, “Holographic derivation of entanglement entropy from AdS/CFT,” *Phys. Rev. Lett.* **96** (2006) 181602, [arXiv:hep-th/0603001 \[hep-th\]](#).
- [4] S. Ryu and T. Takayanagi, “Aspects of Holographic Entanglement Entropy,” *JHEP* **08** (2006) 045, [arXiv:hep-th/0605073 \[hep-th\]](#).
- [5] A. Kapustin and E. Witten, “Electric-Magnetic Duality And The Geometric Langlands Program,” *Commun. Num. Theor. Phys.* **1** (2007) 1–236, [arXiv:hep-th/0604151 \[hep-th\]](#).
- [6] T. Azeyanagi, A. Karch, T. Takayanagi, and E. G. Thompson, “Holographic calculation of boundary entropy,” *JHEP* **03** (2008) 054–054, [arXiv:0712.1850 \[hep-th\]](#).
- [7] M. Chiodaroli, M. Gutperle, L.-Y. Hung, and D. Krym, “String Junctions and Holographic Interfaces,” *Phys. Rev.* **D83** (2011) 026003, [arXiv:1010.2758 \[hep-th\]](#).
- [8] M. Chiodaroli, M. Gutperle, and L.-Y. Hung, “Boundary entropy of supersymmetric Janus solutions,” *JHEP* **09** (2010) 082, [arXiv:1005.4433 \[hep-th\]](#).
- [9] J. Estes, K. Jensen, A. O’Bannon, E. Tsatis, and T. Wrase, “On Holographic Defect Entropy,” *JHEP* **05** (2014) 084, [arXiv:1403.6475 \[hep-th\]](#).
- [10] E. D’Hoker and M. Gutperle, “Holographic entropy and Calabi’s diastasis,” *JHEP* **10** (2014) 93, [arXiv:1406.5124 \[hep-th\]](#).
- [11] M. Gutperle and J. D. Miller, “Entanglement entropy at holographic interfaces,” [arXiv:1511.08955 \[hep-th\]](#).
- [12] K. Jensen and A. O’Bannon, “Holography, Entanglement Entropy, and Conformal Field Theories with Boundaries or Defects,” *Phys. Rev.* **D88** no. 10, (2013) 106006, [arXiv:1309.4523 \[hep-th\]](#).

- [13] H. Casini, M. Huerta, and R. C. Myers, “Towards a derivation of holographic entanglement entropy,” *JHEP* **05** (2011) 036, [arXiv:1102.0440 \[hep-th\]](#).
- [14] J. M. Maldacena, “Wilson loops in large N field theories,” *Phys. Rev. Lett.* **80** (1998) 4859–4862, [arXiv:hep-th/9803002 \[hep-th\]](#).
- [15] S.-J. Rey and J.-T. Yee, “Macroscopic strings as heavy quarks in large N gauge theory and anti-de Sitter supergravity,” *Eur. Phys. J.* **C22** (2001) 379–394, [arXiv:hep-th/9803001 \[hep-th\]](#).
- [16] J. Gomis and F. Passerini, “Holographic Wilson Loops,” *JHEP* **08** (2006) 074, [arXiv:hep-th/0604007 \[hep-th\]](#).
- [17] J. Gomis and F. Passerini, “Wilson Loops as D3-Branes,” *JHEP* **01** (2007) 097, [arXiv:hep-th/0612022 \[hep-th\]](#).
- [18] S. Yamaguchi, “Wilson loops of anti-symmetric representation and D5-branes,” *JHEP* **05** (2006) 037, [arXiv:hep-th/0603208 \[hep-th\]](#).
- [19] E. D’Hoker, J. Estes, and M. Gutperle, “Gravity duals of half-BPS Wilson loops,” *JHEP* **06** (2007) 063, [arXiv:0705.1004 \[hep-th\]](#).
- [20] S. Yamaguchi, “Bubbling geometries for half BPS Wilson lines,” *Int. J. Mod. Phys.* **A22** (2007) 1353–1374, [arXiv:hep-th/0601089 \[hep-th\]](#).
- [21] O. Lunin, “On gravitational description of Wilson lines,” *JHEP* **06** (2006) 026, [arXiv:hep-th/0604133 \[hep-th\]](#).
- [22] S. A. Gentle and M. Gutperle, “Entanglement entropy of Wilson loops: Holography and matrix models,” *Phys. Rev.* **D90** no. 6, (2014) 066011, [arXiv:1407.5629 \[hep-th\]](#).
- [23] S. Gukov and E. Witten, “Gauge Theory, Ramification, And The Geometric Langlands Program,” [arXiv:hep-th/0612073 \[hep-th\]](#).
- [24] S. Gukov and E. Witten, “Rigid Surface Operators,” *Adv. Theor. Math. Phys.* **14** no. 1, (2010) 87–178, [arXiv:0804.1561 \[hep-th\]](#).
- [25] J. Gomis and S. Matsuura, “Bubbling surface operators and S-duality,” *JHEP* **06** (2007) 025, [arXiv:0704.1657 \[hep-th\]](#).
- [26] H. Lin, O. Lunin, and J. M. Maldacena, “Bubbling AdS space and 1/2 BPS geometries,” *JHEP* **10** (2004) 025, [arXiv:hep-th/0409174 \[hep-th\]](#).

- [27] H. Lin and J. M. Maldacena, “Fivebranes from gauge theory,” *Phys. Rev.* **D74** (2006) 084014, [arXiv:hep-th/0509235 \[hep-th\]](#).
- [28] A. Lewkowycz and J. Maldacena, “Generalized gravitational entropy,” *JHEP* **08** (2013) 090, [arXiv:1304.4926 \[hep-th\]](#).
- [29] S. A. Gentle, M. Gutperle, and C. Marasinou, “Entanglement entropy of Wilson surfaces from bubbling geometries in M-theory,” *JHEP* **08** (2015) 019, [arXiv:1506.00052 \[hep-th\]](#).
- [30] O. J. Ganor, “Six-dimensional tensionless strings in the large N limit,” *Nucl. Phys.* **B489** (1997) 95–121, [arXiv:hep-th/9605201 \[hep-th\]](#).
- [31] D. E. Berenstein, R. Corrado, W. Fischler, and J. M. Maldacena, “The Operator product expansion for Wilson loops and surfaces in the large N limit,” *Phys. Rev.* **D59** (1999) 105023, [arXiv:hep-th/9809188 \[hep-th\]](#).
- [32] R. Corrado, B. Florea, and R. McNees, “Correlation functions of operators and Wilson surfaces in the $d = 6$, $(0,2)$ theory in the large N limit,” *Phys. Rev.* **D60** (1999) 085011, [arXiv:hep-th/9902153 \[hep-th\]](#).
- [33] E. Witten, “Some comments on string dynamics,” in *Future perspectives in string theory. Proceedings, Conference, Strings’95, Los Angeles, USA, March 13-18, 1995*. 1995. [arXiv:hep-th/9507121 \[hep-th\]](#).
- [34] A. Strominger, “Open p-branes,” *Phys. Lett.* **B383** (1996) 44–47, [arXiv:hep-th/9512059 \[hep-th\]](#).
- [35] E. D’Hoker, J. Estes, M. Gutperle, and D. Krym, “Exact Half-BPS Flux Solutions in M-theory. I: Local Solutions,” *JHEP* **08** (2008) 028, [arXiv:0806.0605 \[hep-th\]](#).
- [36] E. D’Hoker, J. Estes, M. Gutperle, and D. Krym, “Exact Half-BPS Flux Solutions in M-theory II: Global solutions asymptotic to $AdS(7) \times S^{*4}$,” *JHEP* **12** (2008) 044, [arXiv:0810.4647 \[hep-th\]](#).
- [37] A. Karch and C. F. Uhlemann, “Generalized gravitational entropy of probe branes: flavor entanglement holographically,” *JHEP* **05** (2014) 017, [arXiv:1402.4497 \[hep-th\]](#).
- [38] C. Holzhey, F. Larsen, and F. Wilczek, “Geometric and renormalized entropy in conformal field theory,” *Nucl. Phys.* **B424** (1994) 443–467, [arXiv:hep-th/9403108 \[hep-th\]](#).

- [39] P. Calabrese and J. L. Cardy, “Entanglement entropy and quantum field theory,” *J. Stat. Mech.* **0406** (2004) P06002, [arXiv:hep-th/0405152 \[hep-th\]](#).
- [40] N. R. Constable, J. Erdmenger, Z. Guralnik, and I. Kirsch, “Intersecting D-3 branes and holography,” *Phys. Rev.* **D68** (2003) 106007, [arXiv:hep-th/0211222 \[hep-th\]](#).
- [41] A. Karch and L. Randall, “Open and closed string interpretation of SUSY CFT’s on branes with boundaries,” *JHEP* **06** (2001) 063, [arXiv:hep-th/0105132 \[hep-th\]](#).
- [42] J. D. Brown and M. Henneaux, “Central Charges in the Canonical Realization of Asymptotic Symmetries: An Example from Three-Dimensional Gravity,” *Commun. Math. Phys.* **104** (1986) 207–226.
- [43] A. Gadde and S. Gukov, “2d Index and Surface operators,” *JHEP* **1403** (2014) 080 [[arXiv:1305.0266 \[hep-th\]](#)].
- [44] B. McClain, F. Yu, and Y. S. Wu, “Covariant quantization of chiral bosons and $\text{OSp}(1,1|2)$ symmetry,” *Nucl. Phys.* **B343** (1990) 689–704.
- [45] C. Wotzasek, “The Wess-Zumino term for chiral bosons,” *Phys. Rev. Lett.* **66** (1991) 129–132.
- [46] I. Martin and A. Restuccia, “Duality symmetric actions and canonical quantization,” *Phys. Lett.* **B323** (1994) 311–315.
- [47] F. P. Devecchi and M. Henneaux, “Covariant path integral for chiral p forms,” *Phys. Rev.* **D54** (1996) 1606–1613, [arXiv:hep-th/9603031 \[hep-th\]](#).
- [48] I. Bengtsson and A. Kleppe, “On chiral p forms,” *Int. J. Mod. Phys.* **A12** (1997) 3397–3412, [arXiv:hep-th/9609102 \[hep-th\]](#).
- [49] N. Berkovits, “Manifest electromagnetic duality in closed superstring field theory,” *Phys. Lett.* **B388** (1996) 743–752, [arXiv:hep-th/9607070 \[hep-th\]](#).
- [50] N. Berkovits, “Local actions with electric and magnetic sources,” *Phys. Lett.* **B395** (1997) 28–35, [arXiv:hep-th/9610134 \[hep-th\]](#).
- [51] P. Pasti, D. P. Sorokin, and M. Tonin, “On Lorentz invariant actions for chiral p forms,” *Phys. Rev.* **D55** (1997) 6292–6298, [arXiv:hep-th/9611100 \[hep-th\]](#).
- [52] G. Dall’Agata, K. Lechner, and D. Sorokin, “Covariant actions for the bosonic sector of $d = 10$ IIB supergravity,” *Class. Quant. Grav.* **14** (1997) L195–L198, [hep-th/9707044 \[hep-th\]](#). <http://arxiv.org/abs/hep-th/9707044>.

- [53] G. Dall’Agata, K. Lechner, and M. Tonin, “D = 10, N = IIB supergravity: Lorentz invariant actions and duality,” *JHEP* **07** (1998) 017, [arXiv:hep-th/9806140 \[hep-th\]](#).
- [54] G. Dall’Agata, K. Lechner, and M. Tonin, “Action for IIB supergravity in 10-dimensions,” [arXiv:hep-th/9812170 \[hep-th\]](#). [Lect. Notes Phys.525,416(1999)].
- [55] A. Sen, “Covariant Action for Type IIB Supergravity,” [arXiv:1511.08220 \[hep-th\]](#).
- [56] M. Henneaux and C. Teitelboim, “Dynamics of Chiral (Selfdual) P Forms,” *Phys. Lett.* **B206** (1988) 650.
- [57] J. H. Schwarz and A. Sen, “Duality symmetric actions,” *Nucl. Phys.* **B411** (1994) 35–63, [arXiv:hep-th/9304154 \[hep-th\]](#).
- [58] D. M. Belov and G. W. Moore, “Type II Actions from 11-Dimensional Chern-Simons Theories,” [arXiv:hep-th/0611020 \[hep-th\]](#).
- [59] S. B. Giddings, S. Kachru, and J. Polchinski, “Hierarchies from fluxes in string compactifications,” *Phys. Rev.* **D66** (2002) 106006, [arXiv:hep-th/0105097 \[hep-th\]](#).
- [60] O. DeWolfe and S. B. Giddings, “Scales and hierarchies in warped compactifications and brane worlds,” *Phys. Rev.* **D67** (2003) 066008, [arXiv:hep-th/0208123 \[hep-th\]](#).
- [61] K. Skenderis and M. Taylor, “Anatomy of bubbling solutions,” *JHEP* **09** (2007) 019, [arXiv:0706.0216 \[hep-th\]](#).
- [62] V. Pestun, “Localization of gauge theory on a four-sphere and supersymmetric Wilson loops,” *Commun. Math. Phys.* **313** (2012) 71–129, [arXiv:0712.2824 \[hep-th\]](#).
- [63] T. Okuda and D. Trancanelli, “Spectral curves, emergent geometry, and bubbling solutions for Wilson loops,” *JHEP* **09** (2008) 050, [arXiv:0806.4191 \[hep-th\]](#).
- [64] J. Gomis, S. Matsuura, T. Okuda, and D. Trancanelli, “Wilson loop correlators at strong coupling: From matrices to bubbling geometries,” *JHEP* **08** (2008) 068, [arXiv:0807.3330 \[hep-th\]](#).
- [65] C. R. Graham and E. Witten, “Conformal anomaly of submanifold observables in AdS / CFT correspondence,” *Nucl. Phys.* **B546** (1999) 52–64, [arXiv:hep-th/9901021 \[hep-th\]](#).

- [66] L.-Y. Hung, R. C. Myers, M. Smolkin, and A. Yale, “Holographic Calculations of Renyi Entropy,” *JHEP* **12** (2011) 047, [arXiv:1110.1084 \[hep-th\]](#).
- [67] K. Jensen and A. O’Bannon, “Constraint on Defect and Boundary Renormalization Group Flows,” *Phys. Rev. Lett.* **116** (2016) no.9, 091601
doi:10.1103/PhysRevLett.116.091601 [[arXiv:1509.02160 \[hep-th\]](#)].
- [68] M. Bill, V. Goncalves, E. Lauria and M. Meineri, “Defects in conformal field theory,”
[arXiv:1601.02883 \[hep-th\]](#).
- [69] I. Papadimitriou and K. Skenderis, “Correlation functions in holographic RG flows,”
JHEP **0410** (2004) 075 doi:10.1088/1126-6708/2004/10/075 [[hep-th/0407071](#)].
- [70] H.-C. Chang and A. Karch, “Entanglement Entropy for Probe Branes,” *JHEP* **01**
(2014) 180, [arXiv:1307.5325 \[hep-th\]](#).
- [71] K. Kontoudi and G. Policastro, “Flavor corrections to the entanglement entropy,”
JHEP **01** (2014) 043, [arXiv:1310.4549 \[hep-th\]](#).